A Metamorphic Study of Pretoria Group Sediments Found at the Dwarsrivier Pass, Bushveld Igneous Complex, South Africa

Submitted in partial fulfilment of the requirements for the degree

MSc Geology

in the department of Geology

University of Pretoria

Nicholas Tweedie Fraser

13030362

25/11/2019

Supervisor: Dr. J. Roberts

DECLARATION OF ORIGINALITY UNIVERSITY OF PRETORIA

I, the undersigned, declare that:

1. I understand what plagiarism is and am aware of the University's policy in this regard.

2. I declare that this research project is my own original work. Where other people's work has been used (from either: a printed source, internet source or any other source), has been properly acknowledged and referenced in accordance with Departmental requirements.

3. I have not used work previously produced by another student or any other person to hand in as my own.

4. I have not allowed, and will not allow, anyone, to copy my work with the intention of passing it off as his or her own work.

SIGNATURE

Nicholas Tweedie Fraser 13030362

Abstract

The study takes place in the Dwarsrivier area which lies on the border between Mpumalanga and Limpopo, to the North-West of Lydenberg, at an exposed road cutting. Within the road cutting, there is a unique portion of exposed rock which is light in colour and identified as a calc-silicate. The calc-silicate material is present as a package of rock and is surrounded top and bottom by pyroxenite. The surrounding rock belongs to the Bushveld Igneous Complex (BIC), which is the largest known layered intrusion on the planet and is host to numerous mines. The sample area is within the Critical Zone of the BIC and the host rock consists of pyroxenite which is crystalline and mafic. The calc-silicate package originates from the Pretoria Group sediments, which hosts the BIC, and has undergone varying degrees of metamorphism and mineralisation. The metamorphism formed and allowed for the preservation of two rare minerals, namely wüstite and chlorospinel. Numerous tests were performed on the samples, including SEM point scans to identify these rare minerals and to better understand how the calc-silicate package was preserved in the BIC. A model was created to explain the occurrence of the calc-silicate slab and surrounding features. The previous model involved the slab rising up through the BIC, but the proposed model in this thesis is that the calc-silicate was part of the roof rock which then delaminated, and subducting into the ductile magma of the BIC.

Acknowledgements

First I would like to thank Dr Roberts for his assistance with and insight of the issues and tasks faced in the completion of this project, I would like to thank the Mineralogy Department at UP for the use of their labs and equipment as well as the Geology Department for the use of their labs and for providing space to work. I want to acknowledge Wiebke Grote (XRD), Carel Coetzee (SEM) and Lebogang Papi (XRF) for their assistance and expertise. I want to thank Kyle Lusted and Francois Lotter for the friendship, laughter and motivation they provided though out. Finally, a special thanks to Shinea Swartz for her unwavering love and support, and her assistance with Coral Draw.

Contents

List of figures

1. Introduction

The road cutting at the top of the Dwarsrivier Pass in the Eastern Limb of the Bushveld Complex features the appearance of sheath folds in igneous layering as well as the presence of a sedimentary xenolith/sheet, and has been visited by numerous geologists and geology field trips over the years. However, the outcrop is relatively undescribed in the geological literature, featuring in only one paper (Clarke et al., 2005) which focused on the igneous portion of the outcrop. This study aims to describe and explain the metasedimentary [EB1] portion of the outcrop in detail, focusing on the origin of the calc-silicate xenolith and the contact metamorphism preserved in this rock. The outcrop is located at 24°56'58.19"S and 30°10'40.49"E as seen in figure 1, which shows the study area's location relative to the Eastern Limb of the BIC.

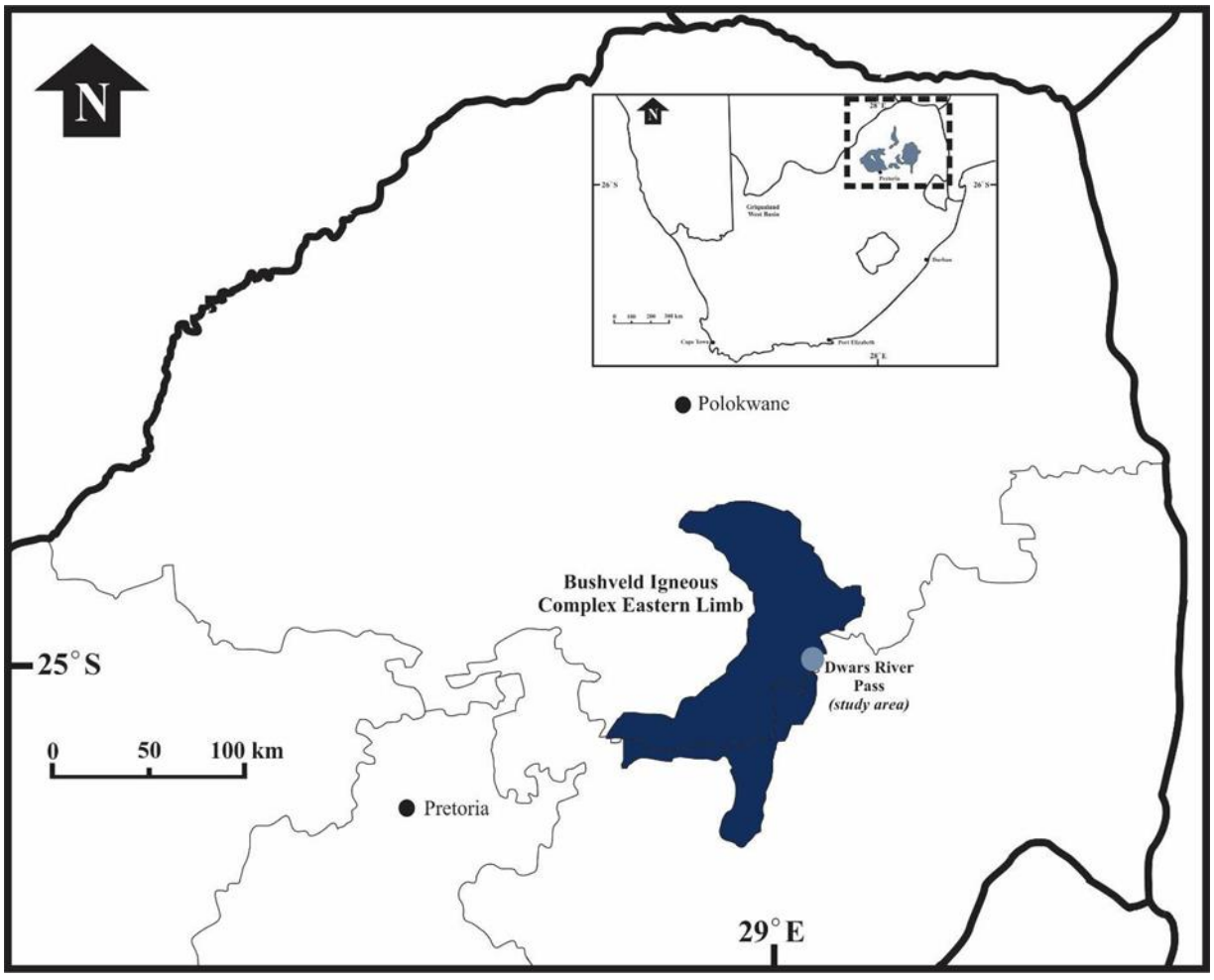

Figure 1: Map showing the location of the study area in relation to the Eastern Limb of the BIC. (Modified after Molyneux, 1974)

1.1 Study Area

The study site for the project is in the Dwarsrivier Pass area, to the south of Steelpoort. Figure 2 is a more detailed map showing the proximity between the sampled area and the assumed contact of the BIC and the Pretoria Group sediments of the Transvaal Supergroup. The outcrop in the road cutting extends for approximately 175m striking NW. The majority of the outcrop consists of mafic igneous rock of the BIC, it is pyroxenite -consisting predominantly of pyroxenes and feldspars[EB2]. The igneous or host rock has as distinct modal distribution of pyroxenes which make fold-like structures which resembles swirls in the rock. These folds occur in different orientations and with different degrees of folding, and some appear recumbent towards the north and others toward the south (Clarke, 2005).

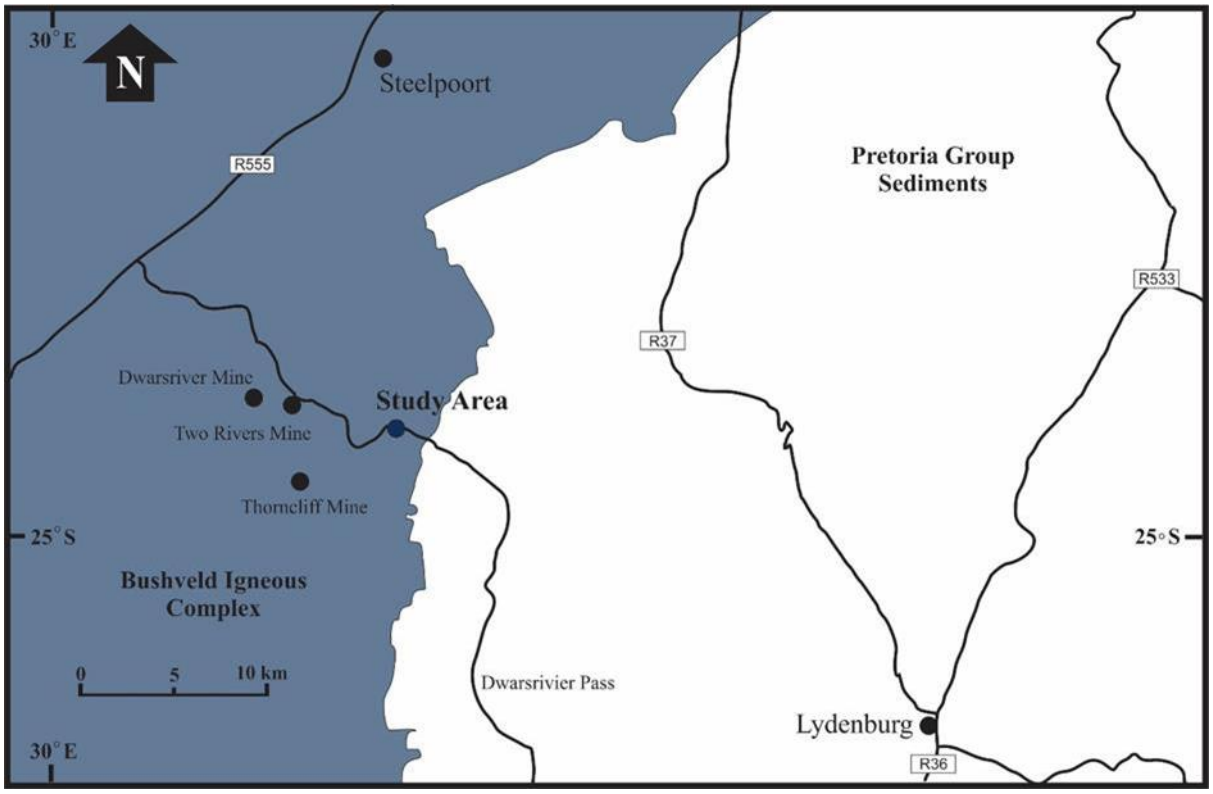

Figure 2: Map of the study area where samples were collected, indicating the boundary between the BIC and Pretoria Group[EB3], Bushveld Igneous Complex (blue), Pretoria Group Sediments (white).

The outcrop from which the samples were collected can be seen in figure 3, which shows the contact between the calc-silicate and the igneous host rock. The calc-silicate is much lighter in colour and ~~clearly~~ -visually different from the surrounding rock. The calc-silicate appears to be a sheet extending to both sides of the road cutting as well as forming the

top portion of the road cutting. The upper portions of the calc-silicate are highly weathered and altered due to exposure and vegetation growth, the lower portions remain relatively fresh. The sheet dips shallowly, between 10° and 15°, [EB4]towards the east and steeply, approximately 45º, towards the west. The steeply dipping portion of the package was the least altered and was the source for the samples collected. The calc-silicate package is 2m thick in this section, with no discernible minerals visible. The package appears to have been layered before metamorphism ~~occurred~~, evident by the alternating light and dark sedimentary sections and fine grain size in ~~e varying textures~~[EB5] ~~and colours of the rock across~~ the profile. The lower portion in contact with the host rock shows evidence of ~~some~~ [EB6]~~re~~crystallisation.~~,~~ M~~m~~oving ~~across~~ from east to west the sample becomes lighter in colour and shows slight foliation. [EB7]The central portion of the package is darker in colour and far harder than the rest of the calc-silicate rock;~~,~~ this may be igneous material that has intruded between sedimentary layers. [EB8]The remainder of the package is light in colour with very fine grains towards the western contact where there is possible recrystallisation present.

It is unlikely that the sedimentary calc-silicate package is part of the BIC as the BIC is consists of mafic igneous rock, with no ~~recorded~~ observed [EB9]carbonatites. The sedimentary package must originate from the neighbouring Pretoria Group and would have been incorporated during the emplacement of the BIC.

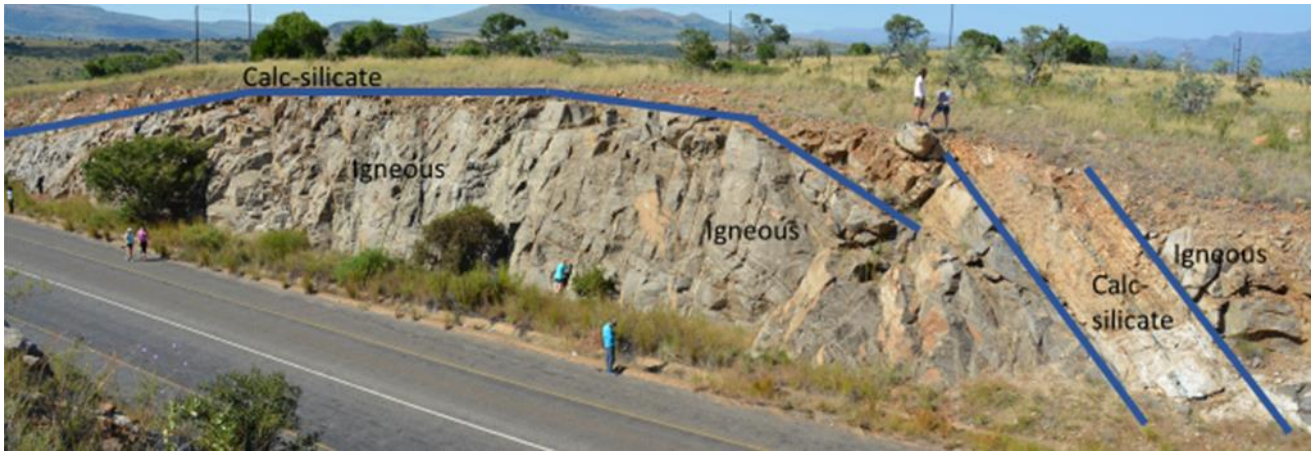

Figure 3: Dwarsrivier Pass road cutting, calc-silicate indicated in blue. Photo by Dr R. Dixon (2017)

1.2 Metamorphism

~~Metamorphism is a process whereby the increase of heat and or pressure causes alteration of the structure, mineralogy and composition of a rock. The term metamorphism originates from the word metamorphosis, a Greek word meaning "to change or alter forms" (Spear, 1995; Bucher and Grapes, 2011). Contact metamorphism occurs in the rock surrounding igneous rock, the area over which the metamorphism has occurred, is called a contact aureole (Bucher and Grapes, 2011). Spear (1995) states that the primary factor that drives the metamorphism is heat from the igneous melt; subsequently the size of the aureole is dependent on the size or volume of the intrusion, the composition of the melt and the country-rock as well as the temperature of the igneous material.~~ [EB10]~~[nf11]~~

The metamorphism caused by the BIC in the Pretoria Group sediments has been studied in other areas of the contact aureole, both along the contact as well as further away from the contact to determine the extent of metamorphism for the entire aureole[EB12]. The contact aureole in the Eastern Limb has been reported by Waters and Lovegrove (2002) to be 4 km thick perpendicular to the contact, which results in a large number of the sedimentary layers undergoing ~~metamorphism to~~ varying degrees[EB13] of metamorphism. [EB14]Nell (1985) suggest that there were two metamorphic events, an initial lower temperature, pressure phase followed by a second higher temperature, pressure phase as the remaining bulk of the BIC was intruded. The first phase of metamorphism occurred at a maximum temperature of 750ºC and a pressure of 0.15 GPa while the second phase occurred at a maximum temperature of approximately 900ºC and a pressure calculated between 0.4 and 0.5 GPa (Nell, 1985). Using garnet based geothermometers and geobarometers Kaneko et al., (2005) calculated metamorphic temperatures ranging from 800ºC near the contact to 450ºC further away from the contact, ~~as low down as the Chuniespoort Group~~ with pressures in the surrounding sedimentary rock ~~Pretoria Group~~ ranging from 0.15 GPa at the contact to 0.3 GPa near the base of the group. [EB15]Waters and Lovegrove (2002) report similar results to Kaneko et al. in 2005, [EB16]and Raubenheimer (2012) calculates similar values for the metamorphism in the distal portions of the aureole. Calc-silicate xenoliths found in the Marginal Zone of the Eastern Limb of the BIC were subjected to metamorphism at temperatures in excess of 1100ºC and pressures of 0.15 GPa which were deduced by mineral assemblages ~~and growth~~ as well as the degree of melting and recrystallisation (Wallmach et al., 1995).

1.3 Aims and Objectives

The thesis aims to measure the grade of metamorphism within the calc-silicate rock and determine the P-T conditions within the BIC at the time of metamorphism. If possible, the origin of the calc-silicate rock will be determined and along with this a working formational model to explain the structure of the rock.

2. Background

2.1 Transvaal Supergroup

The Transvaal Supergroup was deposited in three separate basins on the Kaapvaal Craton over approximately 620 million years, between 2,670 Ga and 2,050 Ga, and each basin contains groups and formations that correlate to the other basins ~~marking significant developments on the planet~~ (Eriksson et al., 1993; Hofmann, 2014). South Africa hosts two of these basins, the Griqualand-West Basin and the Transvaal Basin. The third basin is the Kanye Basin in Botswana, which is considered an extension of the Griqualand-West by Moore (2001). Figure 4 displays the location and relation between the three basins. There are three major units that correlate between each of the basins all separated by unconformities (Hofmann, 2014), with the Transvaal Basin including an additional two units that consist of clastic sediments and volcanics.

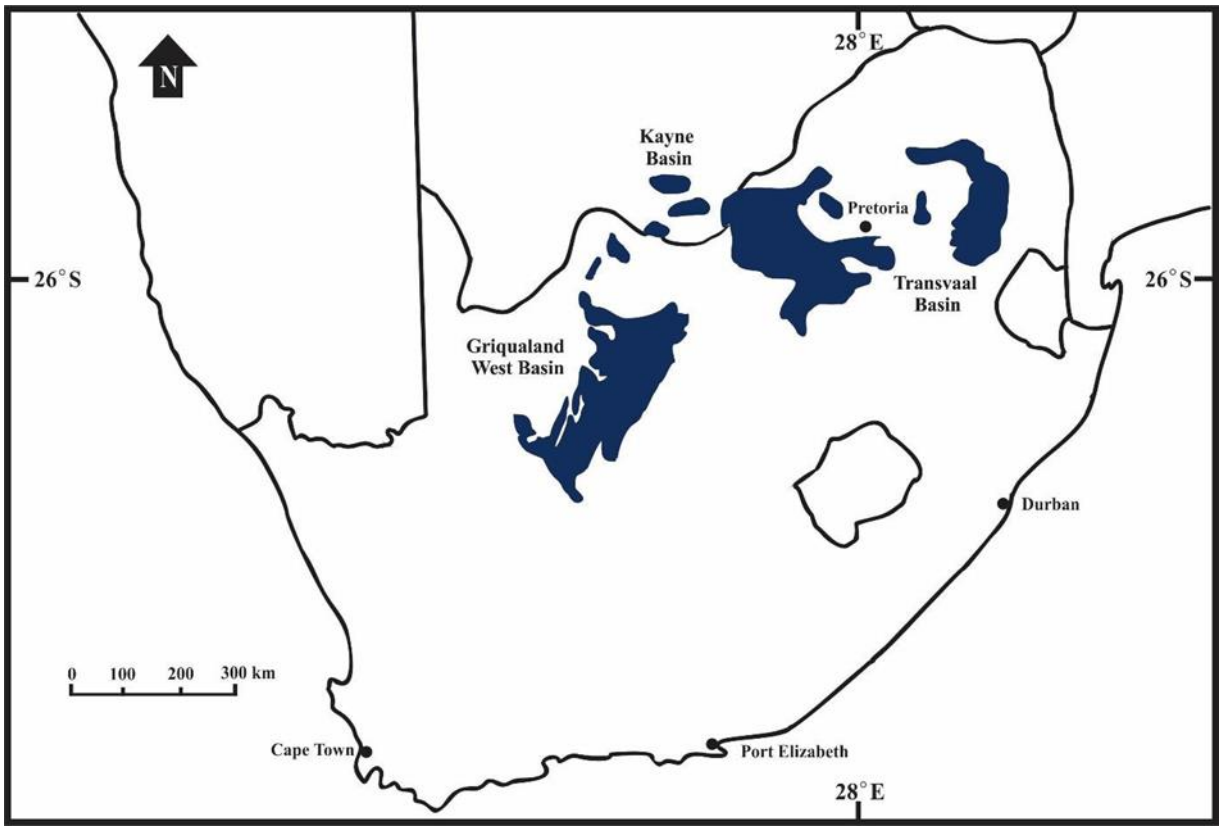

Figure 4: Map representing the three basins in which the Transvaal Supergroup was deposited (Modified after Eriksson et al., 2001)

The base of the Transvaal Basin consists of groups that contain protobasinal rock, and the Rooiberg Group makes up the top of the basin (Eriksson et al., 2001). The bottom correlating unit consists of quartz arenites, the Black Reef Formation in both the Kanye and Transvaal basins and the Vryberg Formation in the Griqualand-WestBasin, the next unit consists of chemical sediments, dolomite and banded iron formations, the Ghaap Group in the Griqualand-West Basin, the Taupone Group in the Kanye Basin and the Chuinespoort Group in the Transvaal Basin (Eriksson et al., 1993). The final corresponding unit is made up of mudrocks, sandstones with occasional volcanic rocks, which are the Postmansberg Group in the Griqualand-West Basin, the Segwagwa Group in the Kanye Basin and the Pretoria Group in the Transvaal Basin (Eriksson et al., 1993). The Pretoria Group has been ~~largely~~ metamorphosed by comparison to the other groups as a result of the intrusion of the BIC (Moore, 2001), and the corresponding units are displayed in figure 5.

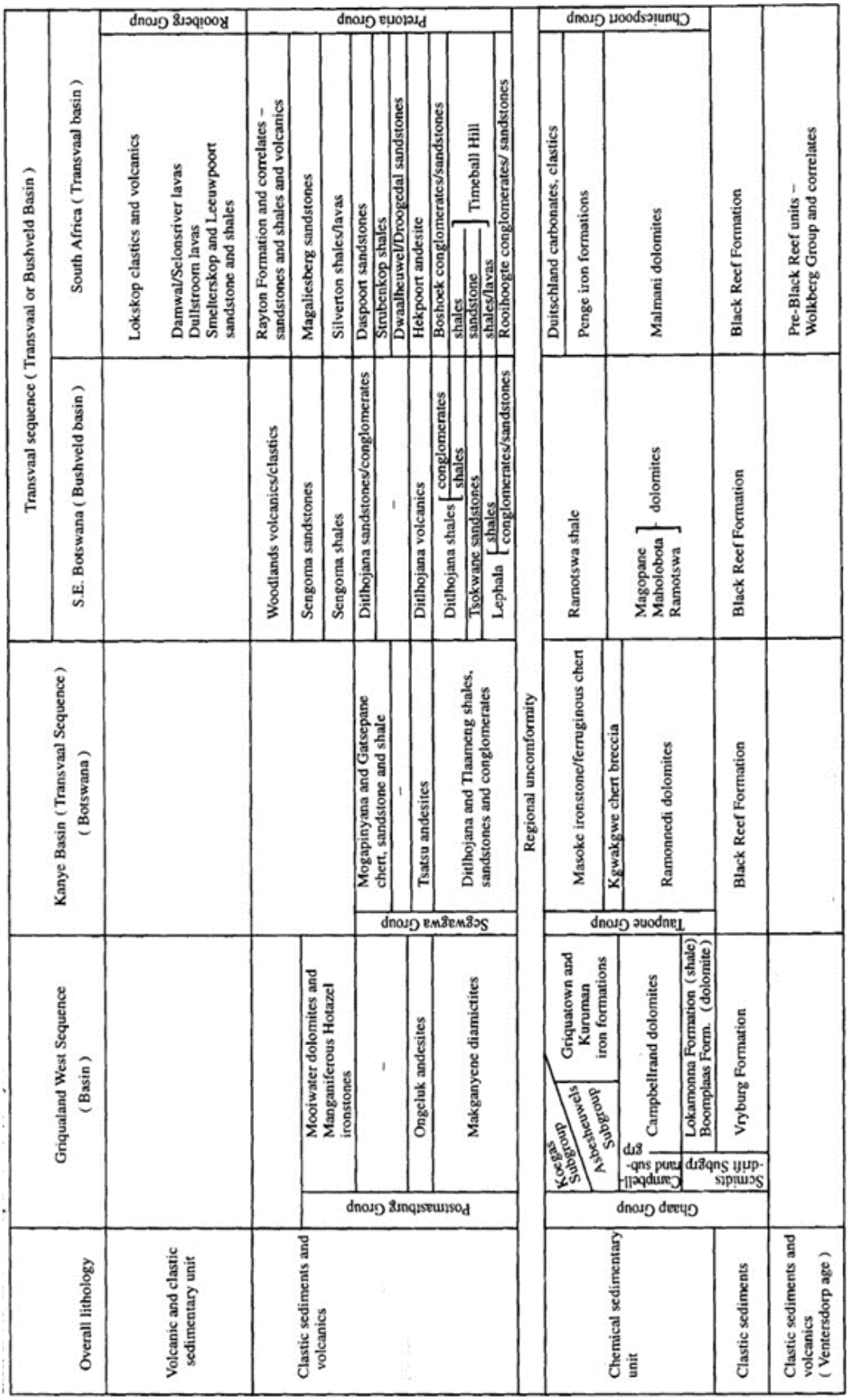

Figure 5: Stratigraphic units of the Transvaal Supergroup represented in the three basins and the corresponding lithologies across each unit (Eriksson et al., 1995a).

2.1.1 Transvaal Basin

The Transvaal Basin is located in the northern part of South Africa with a small section in the southern part of Botswana (Moore, 2001), locally known as the Bushveld Basin. The lithologies in the two basins [EB17]are the same but have been named differently based on the location (Eriksson et al., 1995b). The Transvaal basin consists of a 15 km parcel made up of sandstones, mudrocks, banded iron formations, dolomites and volcanics divided into the before mentioned groups (Eriksson et al., 1993). The initial protobasin was formed by an extensional event which Eriksson et al. (2001) linked to the Ventersdorp Supergroup mantle plume. After the eruption and deposition of the protobasinal groups the basin is thought to have undergone thermal subsidence which allowed for the fluvial sediments of the Black Reef Formation to be deposited and later, with global sea-level rise, the deeper chemical sediments of the Chuniespoort Group (Eriksson et al., 1993). The unconformity between the Pretoria Group and the Chuniespoort Group is caused by a period of regional uplift and reduced sedimentation, followed by two cycles of rifting and subsidence during which the Pretoria Group sediments were provided with an epeiric sea to be deposited in (Eriksson et al., 2001). The Rooiberg Group rocks of the BIC succeeded the deposition of the Pretoria Group (Eriksson et al., 1988), and the Rustenberg Layered Suite (RLS) then intruded into the Pretoria Group resulting in the metamorphism of the rocks (Eriksson et al., 1987). A full stratigraphy of the Transvaal sequence within the Transvaal basin can be seen in figure 6.

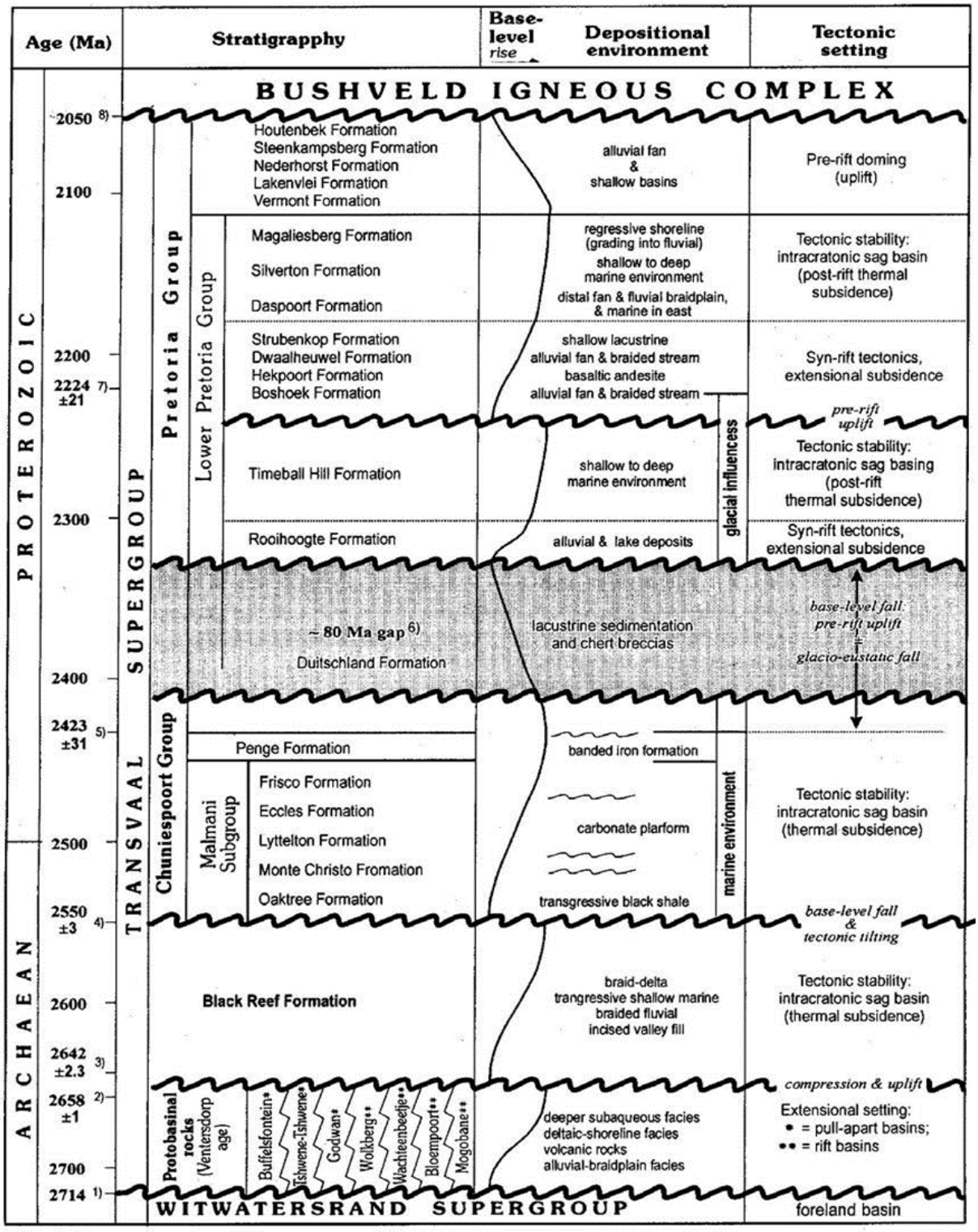

Figure 6: Stratigraphy of the Transvaal Basin (Eriksson et al., 2001)

2.2 Pretoria Group

The Pretoria Group is host to the BIC contact aureole and has undergone varying degrees of metamorphism (Button, 1976; Water and Lovegrove, 2002). The Pretoria Group is predominantly made up of alternating layers of mudstones and quartzitic sandstones with a few prominent layers of andesitic-basaltic lava. It also contains minor, carbonate, arkose and conglomerate rocks (Eriksson et al., 1988; Schrieber et al.,1992). The basal formation in the Pretoria Group, which lies unconformably on the Chuniespoort Group, is the Rooihoogte Formation which composed of quartzites, shales, conglomerates and chert breccias (Catuneanu and Eriksson, 2002). The overlying unit is the Timeball Hill Formation which contains the Bushy Bend Lava member (Lenhardt et al., 2012) as well as shales and sandstone. Both the Timeball Hill and Rooihoogte formations are associated with glacial influence with an unconformity capping the Timeball Hill Formation (Catuneanu and Eriksson, 2002). The Boshoek Formation overlies the Timeball Hill Formation, made mostly of sandstones and conglomerates (Eriksson et al., 1993), followed by the basaltic-andesite lavas of the Hekpoort Formation (Catuneanu and Eriksson, 2002). The Dwaal Heuwel is the next formation in the Pretoria Group consisting of quartzites. The Dwaal Heeuwel is overlain by the shale and minor quartzite layers of the Strubenkop Formation. The Strubenkop Formation underlies the quartzites of the Daspoort Formation (Schrieber et al.,1992; Eriksson et al., 1993).

The next units in the Pretoria Group are in contact with the BIC according to Button (1976), and the relation between the BIC and the Pretoria Group sediments of the Transvaal Supergroup[EB18] can be seen in figure 7. The Silverton Formation consists of shales and volcanic rocks. The Magaliesberg Formation which consists mostly of metamorphosed sandstones overlies the Silverton Formation, with the Rayton Formation forming the top unit. The Rayton Formation consists of shales, quartzites and volcanic rock (Eriksson et al., 1993), and is found in the central portion of the Transvaal Basin. Towards the east of the basin the layers of the Rayton Formation are separated into five unique formations (Eriksson et al., 1988). The five formations are the Vermont Formation, Lakenvalei Formation, Nederhorst Formation, Steenkampsberg Formation and the Houtenbek Formation (Button, 1976; Schrieber et al., 1992).

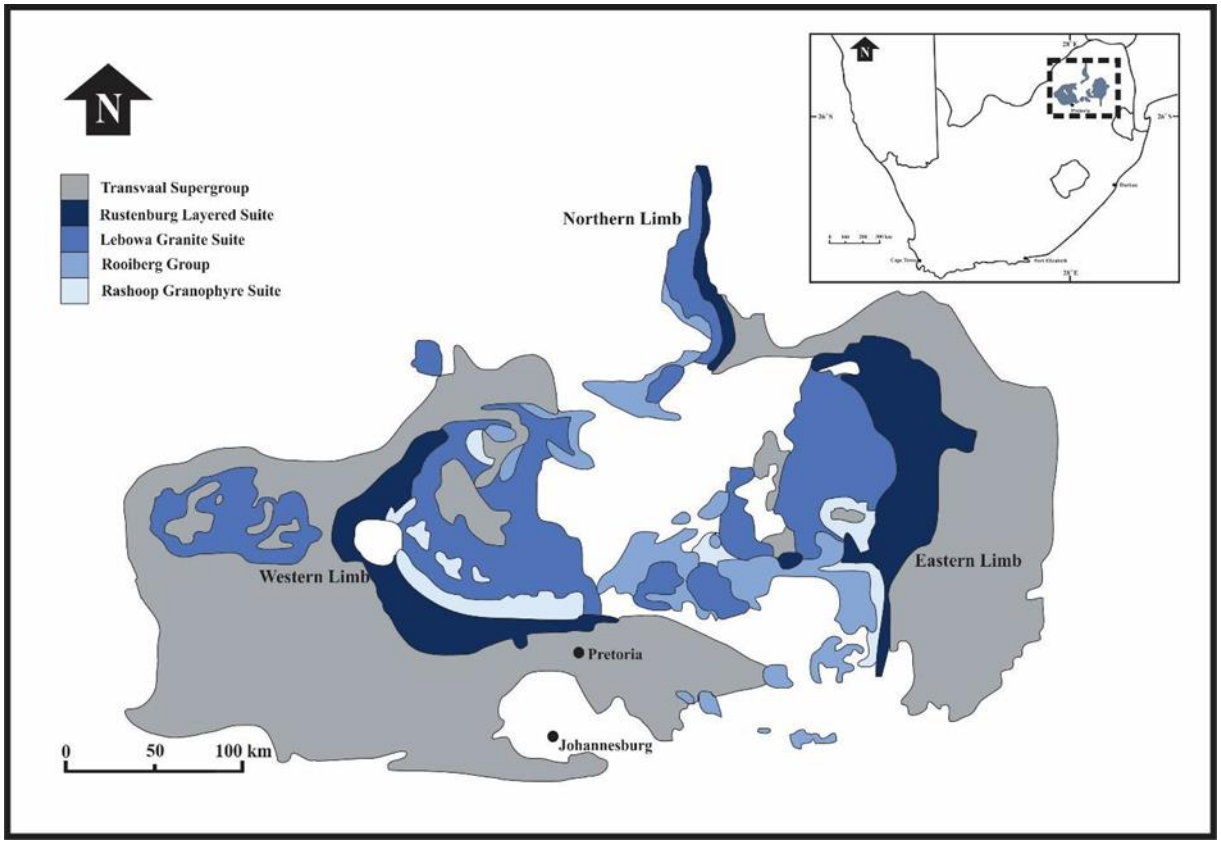

Figure 7: Map of the BIC surrounded by Transvaal Supergroup sediments, (modified after Kinnaird, 2005)

2.2.1 Silverton Formation

The Silverton Formation varies largely in thickness across the different sections of the Transvaal Basin, and in the east, it is estimated at 2500 m thick (Eriksson et al., 1990) formed in an epeiric sea, a transgressive marine environment (Eriksson et al., 1993). The Silverton Formation is comprised of three members, namely the Boven shales ± 250 m, Machadodorp volcanics ± 500 m and the Lydenberg shales ± 1700 m (Eriksson et al., 1993; Reczko, 1995). The Boven shales underlie the Machadodorp volcanics and comprise of carbonaceous mudrocks that are commonly metamorphosed to slates and hornfelses by the intrusion of the BIC (Eriksson et al., 1990). The Boven shales end with the deposition of an upward coarsening sequence of volcaniclastic rocks, from fine-grained tuff to fluvial clast breccias which according to Lenhardt et al. (2012) is the base of the Machadodorp volcanic member. Lenhardt et al. (2012) reports that the volcanoclastic rocks are overlain by dark grey sheet-like lavas. The uppermost member of the Silverton Formation is the Lydenberg shales which consist of varying layers of greenish shales with thin non-continuous layers of limestones, tuff and carbonates (Button, 1976).

For the shales in the Silverton Formation, samples were taken by Eriksson et al. (1990) in order to identify the minerals present and the overall mineralogy of the shales. These shales consist of quartz, plagioclase, biotite, muscovite with carbonaceous material as well as iron oxides. The shales also contained minor quantities of cordierite, chlorite, K- feldspar and hornblende (Eriksson et al., 1990). The volcanic portion of the Silverton Formation consisted of a fine matrix made of tremolite – actinolite and epidote with microphenocrysts of clinopyroxene, olivine and plagioclase in the matrix (Lenhardt et al., 2012).

2.2.2 Magaliesberg Formation

The Magaliesberg Formation grades gradually from the shales of the Silverton Formation into predominantly medium-grained arenite and fine-grained argillite (Button, 1976). In the east of the Transvaal Basin, the Magaliesberg Formation is recorded by Eriksson et al. (1995a) with a thickness of 500 m while other sections of the formation range in thickness between 200 m and 350 m. Button (1976) reports the depositional environment as a shallow marine shelf due to the presence of well- preserved sedimentary structures such as cross-beds and ripple marks, later work done by Eriksson et al. (1993) suggests that the environment is more likely the shore region of a transgressional epeiric sea that has been subjected to reworking by fluvial processes. It is common for the quartz-rich sandstones, which dominate this formation, to be recrystallised due to metamorphism caused by the BIC (Eriksson et al., 1995a). The metamorphism is also responsible for the destruction of fine structures in the rocks. The majority of the formation consists of quartz-rich sandstones or quartzites, making quartz the primary mineral present with minor other minerals present such as muscovite and microcline (Parizot et al., 2006). The Magaliesberg Formation grades upwards into the overlying formation with alternating layers of impure quartzites, quartz wacke, shales and siltstones (Button, 1976).

2.2.3 Vermont Formation

The Vermont Formation consists predominantly of mudrock with gradational contacts both above and below the formation (Schrieber and Eriksson, 1992), ranging between 480 m and 700 m in thickness (Button, 1976). The upper portion of the formation displays characteristics of being deposited in tidal mudflats whereas the middle and lower sections

were deposited in deeper water (Button, 1976). Schrieber and Eriksson (1992) identified cross-bedding, ripple marks, mud cracks and channel filling in the formation. Large portions of the Vermont Formation have been metamorphosed by the intrusion of the BIC as well as intruding dykes (Button, 1976).Schrieber and Eriksson (1992) describe a division of the mudrock into thin layers rich in silt and thick layers rich in mud, as well as localised carbonate rock. Button (1976) encountered similar carbonate rocks and chert in three sections of the formation, 100 m to 150 m from the base of the formation, towards the middle of the formation and 80m to 100m from the top of the formation. Button (1976) found that the sections of carbonate and chert are often metamorphosed to marble, serpentinised dolomite and calc-silicate rocks.

2.2.4 Lakenvalei Formation

The Lakenvalei Formation grades gradually from the shales of the Vermont Formation, coarsening upwards, into fine to medium-grained sandstones. T~~,~~ the formation is roughly 160 m thick towards the north and thickens to 300 m in the south [EB19](Button, 1976). As a result of the [EB20]intrusion of the BIC, the subarkose sandstones of the formation, which form the majority of the unit (Schrieber and Eriksson, 1992), have begun recrystallising, forming felspathic quartzites which occur in cyclic units (Button, 1976). Schrieber and Eriksson (1992) describe planar, trough and herringbone cross-beds as present in the formation as well as ripple marks. The structures are due to the depositional environment which Button (1976) postulates is an area of interaction between a braided delta environment and an interface complex, foreshore environment. A sharp contact with the Nederhorst Formation caps the Lakenvalei Formation (Schrieber and Eriksson, 1992).

2.2.5 Nederhorst Formation

The Nederhorst Formation has a lower unit comprising of hornfels formed through the metamorphism of mudrock with interbedded dolomites and an upper unit comprising of fine-grained arkose to quartzitic sandstones (Button, 1976; Schrieber and Eriksson, 1992). The formation is 800 m thick to the south, thinning to 200 m in the north (Button, 1976)~~,~~. The thinning~~this~~ is accompanied by a change in the upper contact, to the south, there is a gradational contact whereas to the north it is a much sharper contact (Schrieber and Eriksson,

1992). [EB21]The lower unit had a depositional environment that was likely tidal mudflats, which includes minor quartzite lenses, as well as calc-silicate rocks in beds that can be up to 5 m thick. The upper unit was most likely the distal portion of a fluvial wedge in which this portion was formed (Button, 1976). There are a large number of mafic sills which split ~~up t~~he formation and cause intrusion breccias. Where this is not the case, minor sedimentary features are preserved such as lenticular bedding and small ripples (Button, 1976; Schrieber and Eriksson, 1992).

2.2.6 Steenkampsberg Formation

The majority of the Steenkampsberg Formation consists of quartzites which are arenaceous to argillaceous in texture, and the formation is observed to have a thickness of between 470 m and 630 m (Button, 1976). Towards the south, the Steenkampsberg Formation has a gradual contact with the Nederhorst Formation transitioning from mudrock to immature sandstones with minor pebbly sandstones near the base. In this area the Steenkampsberg Formation is directly in contact and overlain by the BIC (Schrieber and Eriksson, 1992).

Further north, the contact with the Nederhorst Formation becomes sharp with a thin basal conglomerate marking the transition. The entire formation contains thin mudrock layers in the central unit ~~of the lithology~~ (Button, 1976). The sediments were deposited in a costal to shallow marine environment displaying the maturing of sediments as well as the fining of grains moving up the formation (Button,1976). Schrieber and Eriksson (1992) observe sedimentary structures such as planar and trough cross-beds with ripple marks, mud cracks and minor channel filling.

2.2.7 Houtenbek Formation

There is a sharp contact between the Houtenbek Formation and the Steenkampsberg Formation with the Houtenbek Formation extending laterally for 50 km. Owing to the large number of intruded sills the thickness is variable ranging between 138 m and 255 m (Button, 1976). The formation consists mainly of metamorphosed mudrock with minor quartzite layers as well as a few carbonate - chert layers containing stromatolites (Schrieber and Eriksson, 1992). It is reported by Schrieber and Eriksson (1992) that within the formation two cyclic

units display upwards coarsening, moving from mudrock to near-perfect quartzites capped by a sharp contact with mudstone and the proceeding cycle. The lower cycle continues for 40 m with the upper cycle only extending for 20 m. Schrieber and Eriksson (1992) found abundant mud cracks, wavy and lenticular bedding in the mudrock facies of the formation. The sandstones in the formation display~~ed~~ planer and trough cross-bedding with pronounced ripple marks. The Houtenbek Formation was likely deposited in a number of coexisting shallow marine environments, such as tidal mudflats, beaches or sub-tidal environments concluded Button (1976). The Houtenbek Formation was superseded by the eruption of the Dullstroom Lavas, the basal unit of the Rooiberg Group (Schweitzer et al., 1995).

2.3 Bushveld Igneous Complex

The Kaapvaal Craton plays host to the BIC in the northern region of South Africa (Cheney and Twist, 1991). The location of the BIC can be seen in figure 8 and formed through the intrusion of magma [EB22]at approximately 2.06 Ga (Walraven et al., 1990). The BIC is considered the largest layered intrusion on the planet, as seen in figure 8 and is comprised predominantly ~~of rock~~ of~~with~~ mafic to ultramafic rock~~compositions~~[EB23] (Latypov et al., 2016). The BIC is divided into three geographical units based on where they outcrop: The Northern Limb, the Western Limb and the Eastern Limb (Eales and Cawthorn, 1996). Within the BIC, there are four major stratigraphic units (Kinnaird, 2005), the Rooiberg Group, the Labowa Granite Suite, the Rashoop Granophyre Suite and the Rustenburg Layered Suite. T~~the~~he top unit is~~being~~ the Rooiberg Group, which was originally assumed to be the upper unit of the Transvaal sequence (Schweitzer et al., 1994). [EB24]The Rooiberg Group consists of large amounts of acidic volcanism which Twist and French (1983) presumed to have been more than 300 000 km^{3}~~?~~ volume[EB25]. It is made up of dacitic and rhyolitic lavas, preserved over an area of approximately 50 000 km^2 (Schweitzer et al., 1994). The Rooiberg Group is divided into four formations starting with the Dullstroom Formation, the lowest unit which overlies the Pretoria Group, followed by the Damwal, the Kwaggasnek and finally the Schrikkloof formations (Schweitzer et al., 1994; Kinnaird, 2005).

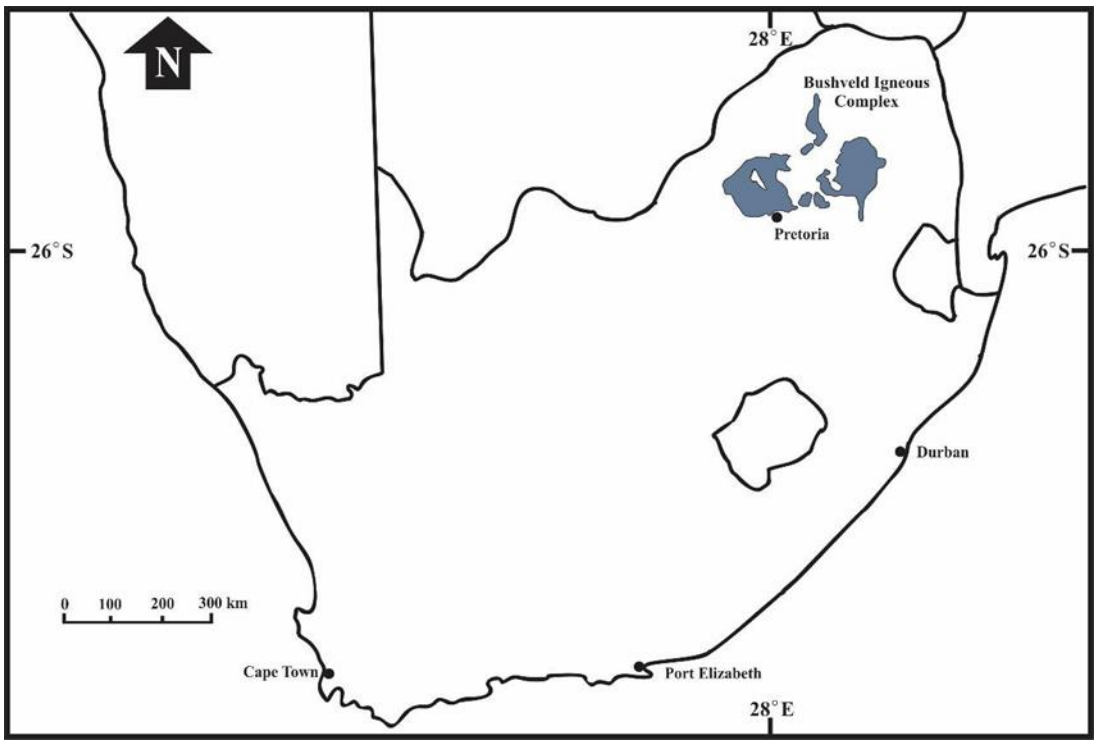

Figure 8: Map showing the location and scale of the BIC

The next unit in the BIC is the Lebowa Granite Suite, the main subunit of which is called the Nebo Granites, which forms the felsic component of the BIC (Wilson et al., 2000). The suite is overlain by the bulk of the Rooiberg Group and overlies the Rustenburg Layered Suite (RLS). According to Kleemann and Twist (1989) the granites were the last unit of the BIC to intrude and did so as slightly dipping sills which form a layer of between 2 km and 3 km thick. These layers are divided into the Makhutso Granite, Nebo Granite, Verena Porphyritic Granit, Klipkloof Granite, Bobbejaankop Granite and the Lease Granite (Eriksson et al., 1995b).

The Rashoop Granophyre Suite is not well documented, and its possible origins include pulses of magma, the recrystallisation of Rooiberg rocks as well as the metamorphism of Pretoria Group sediments (Walraven, 1985). [EB26]The rocks have been grouped based on texture despite the various origins (Kinnaird, 2005). The Rashoop Granophyres have been divided into four units described by Walraven (1985) as the Zwartbank Pseudogranophyre, Diepkloof Granophyre, Stavoren Granophyre and the Rooikop Porphyry.

2.3.1 Rustenburg Layered Suite

The final unit of the BIC is the Rustenberg Layered Suite (RLS) which intruded as sill-like layers into the sediments of the Pretoria Group (Kinnaird, 2005). The RLS is in contact with the sediments of the Pretoria Group, making it the primary cause for the metamorphism of the sediments (Waters and Lovegrove, 2002). The RLS spans a calculated area of 65 000 km^2 [EB27] (Eales and Cawthorn, 1996), with an approximate average thickness reported by Cawthorn and Walraven (1998) of 6 km with a maximum thickness of 8 km in the Eastern Limb of the BIC. The intrusion is a result of multiple pulses of magma of varying volumes (Cawthorn and Walraven, 1998).~~,~~ A~~a~~s a result of the pulses and differentiation of the magma, the RLS is divided into several units (Eales et al., 1993 and 1996). [EB28]The Marginal Zone is the lowest unit of the RLS and is not present everywhere; where it is present, it forms the basal contact with the Pretoria Group (Kinnaird, 2005). It ranges in thickness from 0 m to 800 m according to Eales and Cawthorn (1996) and is ~~comprises~~[EB29] predominantly comprised of norites with medium grains, smaller than the rest of the RLS (Eales et al., 1993). The Lower Zone lies on top of the Marginal Zone ranging in thickness from 800 – 1300 m (Barnes and Maier, 2002), containing pyroxenite, harzburgite and dunite. The Lower Zone is overlain by

the Critical Zone (Eales and Cawthorn, 1996; Cawthorn and Walraven, 1998). The Critical Zone is divided into an upper and lower portion with the boundary marked by the first appearance of plagioclase bearing rock in the Eastern Limb, norite and anorthosite (Eales et al., 1993). In the lower portion, the rocks form bands of alternating pyroxenites and numerous chromitites. In the upper portion the altering layers include the norites and anorthosites (Cawthorn and Walraven, 1998; Barnes and Maier, 2002). The overlying unit is the Main Zone; the Merensky Reef marks the boundary between the lower and main zones (Cawthorn and Walraven, 1998). ~~and~~ The unit is made of norites at the bottom grading into gabbronorites up the unit (Eales et al., 1993). [EB30]The Main Zone is the thickest unit, in excess of 3 km thick and consists of two unique pulses separated by the Pyroxenite Marker (Cawthorn and Walraven, 1998). The last unit in the RLS is the Upper Zone which is on average 2 km thick and displays good layering; the base is marked by the presence of magnetite rich layers (Eales and Cawthorn, 1996). The zone consists of interlayered magnetites, anorthosites and gabbronorites with the top section in contact with the felsites or granophyres made of diorite (Barnes and Maier, 2002).

The heat from the intruding RLS drove the metamorphism of the Pretoria Group. ~~,~~ Studies have been performed to calculate the original temperatures of the magma at the time of intrusion as well as the rate of cooling for the body.[EB31] Cawthorn and Walraven (1998) suggest that the RLS was emplaced at a rate in excess of 9 km^3/ year for approximately 75 000 years, and that the RLS took 200 000 years to crystallise in total, starting from 1300ºC. After crystallisation, the top of the RLS was calculated to be approximately 900ºC with the base at approximately 650ºC. Cawthorn and Webb (2013) states that the temperature gradient at the basal contact of the intrusion was 100ºC / km. Cawthorn and Webb (2013) suggest that the RLS cooled to below the Curie point in approximately 700 000 years based on palaeomagnetism, whereas Zeh et al. (2015) using zircons found in the central portion of the RLS calculated between 600 000 and 950 000 years for the RLS to cool below 700ºC.

3. Methodology

3.1 Sample Collection

Samples were collected from a road cutting located on the Dwarsrivier Pass, seen in figure 3 and 9. The Pass is between Steelpoort and Lydenberg, the site is to the East of the Thorncliff, Two Rivers and Dwarsrivier mines. The location of the study area relative to these locations can be seen in figure 2. For the study, samples were collected across the width of the sedimentary parcel as well as from the neighbouring igneous material, using ~~a sledgehammer~~a sledgehammer to dislodge the samples from the source rock. There were six samples taken in total, five of which came from the sedimentary parcel namely samples NF-01, NF-02, NF-03, NF-04 and NF-05 with a sample taken from the surrounding igneous rock, NF-06. The locations of samples NF-01 to NF-05 can be seen in figure 9. Sample NF- 06 was taken further away from the calc-silicate slab, to ensure that it was an unaltered sample of the host rock.

Figure 9: Sample area of calc-silicate samples collected across the slab, person on right of image is 1,9m tall.

3.2 Sample Preparation

A diamond-tipped saw was used to cut samples into smaller blocks; small pieces of each sample were set aside for thin section production. The remaining samples were milled using a single unit swing mill in a tungsten-carbide milling pot. Each sample was milled for 2 min with some samples requiring a further 2 min to ensure the correct consistency. Every sample was then divided evenly for both X-ray diffraction and X-ray fluorescence spectroscopy.

3.3 Thin Sections

Each sample had two polished thin sections made from alternative sides of the sample, excluding samples NF-06 which had thin sections made of specific sections. The thin sections were named accordingly NF-01-T and NF-01-B, NF-02-T and NF-02-B, NF-03-T and NF-03-B, NF-04-B and NF-04-1, and NF-05-1 and NF-05-2, NF-06-A and NF-06-B. Thin sections were made at Wits University, mounted on glass and ground to a thickness of 0.3 mm using both a LOGITECH machine as well as by hand.

3.4 X-ray Fluorescence Spectroscopy

Samples were sent to UIS Analytical Services for X-ray fluorescence spectroscopy (XRF) to determine the major element chemistry for all samples. UIS uses an “ARL ADVANT'X SERIES” machine utilising the fusion technique of XRF, lithium tetraborate ($Li_2B_4O_7$) was used as a flux.

3.5 Scanning Electron Microscope

Individual thin sections were analysed in the Scanning Electron Microscope (SEM) for point-based chemical compositions using a JOEL JSM-IT300. A tungsten filament was used for the scans, and the vacuum chamber was at low vacuum to prevent the charging of the thin section. The analysis and results presented and compiled with the Oxford system. The thin sections were not coated to ensure accurate results.

4. Results

4.1 XRF (Major Elements)

Table 1 displays the bulk rock chemistry for each of the samples. Samples NF-01 and NF-06 are considered igneous in origin, and have high FeO and SiO_2 values when compared to the other samples; in contrast, these same samples have very low amounts of CaO compared to the other samples. The other samples are distributed across the xenolith sheet. All the samples collected have MgO wt% within 10% of each other, as well as the Al_2O_3 wt% which for each sample is within 4 wt% excluding sample NF-03. NF-03 has the highest amount of CaO present with very little FeO or Al_2O_3 and it is the most calcium-rich sample in the package. Samples NF-03 and NF-05 have very low totals and have reported LOI (loss on ignition) values of 8,759 and 10,050 respectively which is likely due to the presence of large amounts of CO_2 in these samples. It is likely that the samples are oxidised, and most of the Fe will be present as Fe_2O_3, which will increase the totals slightly. NF-04 displays increased SiO_2, FeO, Na_2O, K_2O and TiO_2 values compared to the neighbouring samples as well as decreased amount of MgO and CaO.

Table 1: Bulk Rock Chemistry in Wt%.						
Oxide Wt%	**NF01**	**NF02**	**NF03**	**NF04**	**NF05**	**NF06**
SiO_2	50,013	33,956	32,126	47,859	30,001	52,686
FeO[EB32]T	6,493	2,825	0,416	3,434	2,511	6,612
MgO	19,796	17,029	14,841	12,635	20,650	21,250
CaO	6,861	33,691	42,641	23,430	26,156	6,029
Al_2O_3	11,013	7,489	0,633	8,512	8,574	9,423
Mn_3O_4	0,171	0,234	0,076	0,099	0,150	0,191
MnO	0,123	0,169	0,055	0,072	0,108	0,137
K_2O	0,681	<0.005	<0.005	0,290	<0.005	0,067
Na_2O	0,704	<0.010	<0.010	0,247	<0.010	0,555
TiO_2	0,111	0,106	0,029	0,267	0,100	0,100
Total	95,966	95,499	90,817	96,846	88,250	97,051
LOI	1,074	2,859	8,759	1,378	10,050	-0,088
Total + LOI	97,041	98,358	99,576	98,223	98,300	96,963

4.2 Sample NF-01

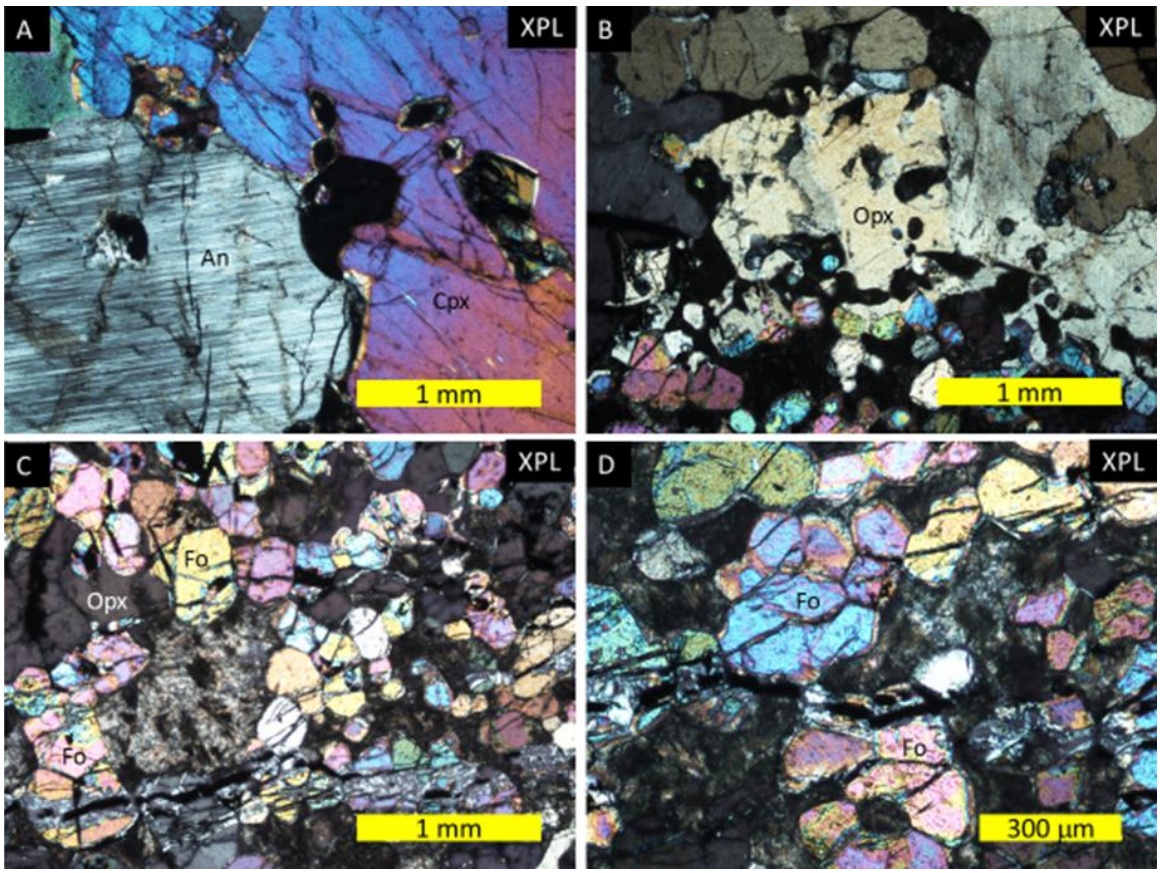

Figure 10: Micrographs of sample NF-01. Fo = Forsterite, An = Anorthite, Opx = Orthopyroxene, Cpx = Clinopyroxene

Sample NF-01 is a gabbro that has been recrystallized, and comes from the lower edge of the sedimentary package. This sample is from the contact between the igneous rock and the sedimentary rock. The thin sections from sample NF-01 show a large variation in grain size from 3000µ~~m~~m in the lower portion, close to the contact, to 150µm[EB33] further away from the contact. Figure 10A shows the lower portion closest to the contact, where there are large 2-3mm anorthite and clinopyroxene crystals. The crystals in the lower portion display poikilitic textures and poor habit with numerous inclusions of small mineral fragments. Figure 10B shows the transition between two prominent textures of the sample, where the large grains are replaced by small forsterite crystals less than 200µm in size as well as an interstitial matrix and minor orthopyroxenes. The last two images (Figures 10C,D) show textures indicative of the majority of the sample, a fine matrix with predominantly small forsterite and orthopyroxene crystals present. The thin section comprises of approximately 20% clinopyroxene, 20% anorthite, 20% orthopyroxene and 30% forsterite. The whole sample comprises of in excess of 60% forsterite as the clinopyroxene and anorthosite are only present near the contact.

4.3 Sample NF-02

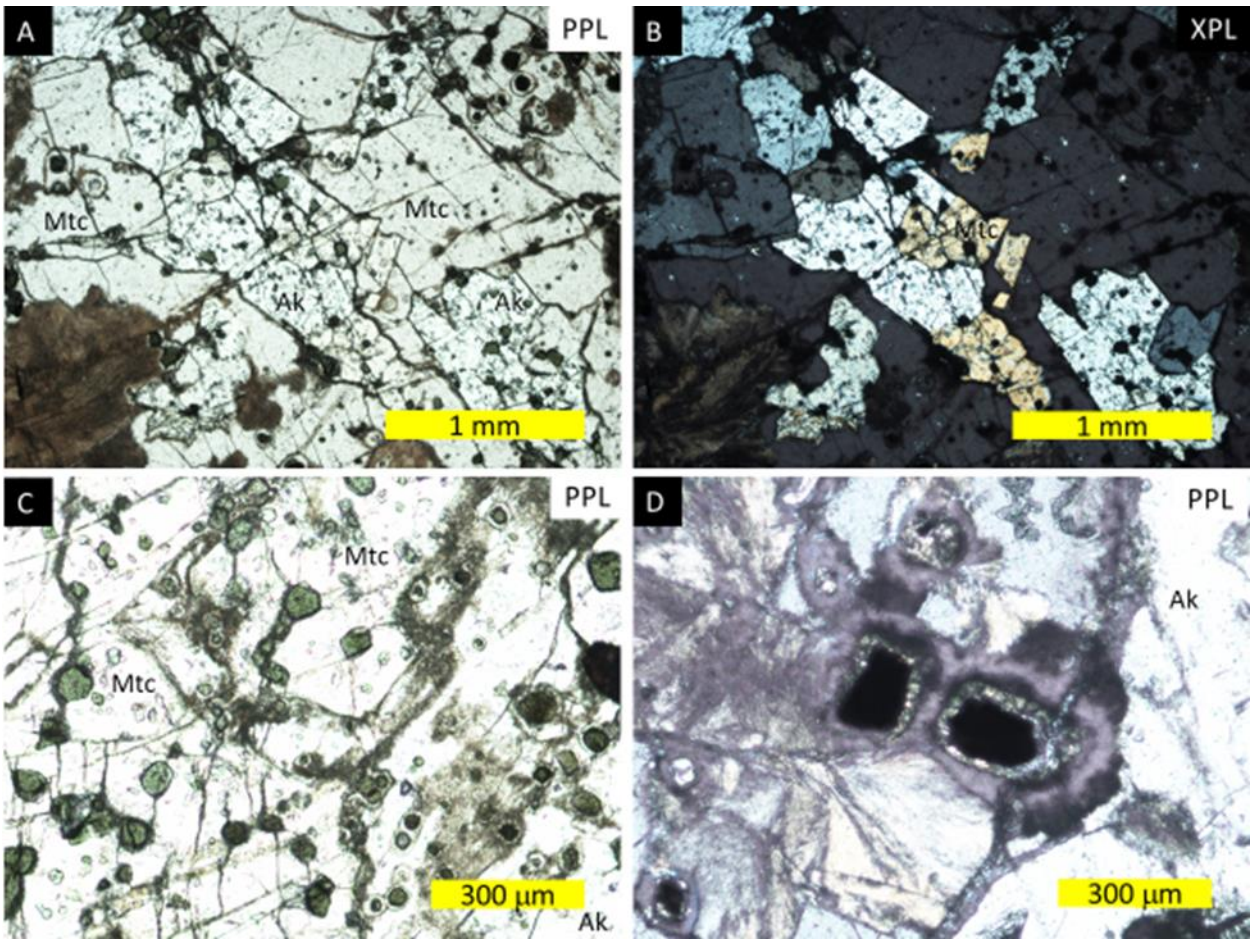

Figure 11: Micrographs of sample NF-02. Ak = Akermanite, Mtc = Monticellite

Sample NF-02 is a metapelite from the second lowest portion of the slab; it comprises mostly of melilites, monticellite, isotropic green minerals and clay minerals as seen in figures 11A,B. The majority of the sample consists of melilite 35% and monticellite 45%, with clay minerals making up 10% and the small included green minerals making up another 10% of the sample. The monticellite crystals are on average between 0.5- 2mm in size and have a subhedral habit. The melilites, which were identified as akermanite, form smaller grains only up to 1.5mm and seem to fill the spaces between the monticellite crystals. Both the monticellite and the akermanite have inclusions of the small 50-200µm isotropic minerals. The green isotropic minerals can be seen more clearly in figure 11C and display euhedral to subhedral shape with occasional reaction rims as seen in Figure 11D. The unknown green minerals were selected for identification with the SEM.

4.3.1 SEM

The unidentified green mineral grains found in the thin sections of sample NF-02 were analysed using the SEM. The analysed minerals have been separated into two groups based on composition. The compositions are presented in tables 2 and 3.

Table 2 shows the minerals that have high FeO wt% in excess of 90 wt% with very little of any other element present. The other elements that are present in the scanned mineral grains are Al, Mn and Zn, none of which exceed 3.6 wt%.

Table 2: Minerals scanned with FeO wt% > 90%

Oxide wt%	Scan 1	Scan 2	Scan 3	Scan 4	Scan 5	Scan 6	Scan 7	Scan 8	Scan 9
FeO^T	93,1	93	91,2	94,2	94,5	94,1	95,2	92,3	93,9
MgO	0	0	0	0,2	0	0,2	0,3	0	0,2
Al_2O_3	2,4	2,2	2,4	0	0,1	0	0	1,8	0,8
SiO_2	0,2	0	0	0,3	0,3	0,4	0,3	0,2	0,2
MnO	2,2	1,8	1,8	2,1	2,4	2	1,6	2,1	2,1
ZnO	2,1	3	3,6	2,1	2,8	2,6	1,9	3,6	2,9
CaO	0	0	0	0	0	0,8	0,6	0	0
Total	100	100	99	98,9	100,1	100,1	99,9	100	100,1

The minerals in Table 3 have been grouped based on high Al_2O_3 wt% in excess of 50 wt%; these minerals also have more than 20 wt% MgO. In two of the scans, the FeO wt% are 28.1 and 24.2 respectively whereas the other three samples have relatively low FeO wt% by comparison. All of these minerals have less than 1 wt% of any other element present.

Table 3: minerals scanned with Al_2O_3 wt% > 50%

Oxide wt%	Scan 1	Scan 2	Scan 3	Scan 4	Scan 5
FeO^T	28,1	24,2	8,3	6,9	6,6
MgO	20,2	21	24,6	25,5	25,6
Al_2O_3	50,5	53,5	66,6	67,4	67,4
SiO_2	0	0	0	0	0
MnO	0	0,8	0,2	0,2	0,2
ZnO	0	0,5	0,3	0	0,2
CaO	0	0	0	0	0,1
Total	98,8	100	100	100	100,1

In Table 2, the scan of the green mineral reveals an extremely large wt% of Fe; this does not correspond with any common minerals for carbonate, calc-silicate or dolomite metamorphism reported by Spear (1995). The mineral is isotropic, ruling out magnetite as the mineral. Both Darken and Gurry (1945), as well as Milodowski et al. (1989), describe a mineral with the composition of FeO that forms and oxidises in CO_2-rich environments; this mineral is wüstite. The other green mineral in question shown in Table 3 consists of Mg, Al, Fe and O; like the wüstite it is also isotropic. The mineral is a chlorospinel described by Bothwell and Hey (1958) as “grass green” with the composition of $MgAl_2O_4$. Chlorospinel can incorporate Fe^{3+} into the lattice, commonly up to 7.2 wt% which corresponds to the mineral analysed in Table 3 (Sabine et al., 1968).

4.3.2 Wüstite and Chlorospinel

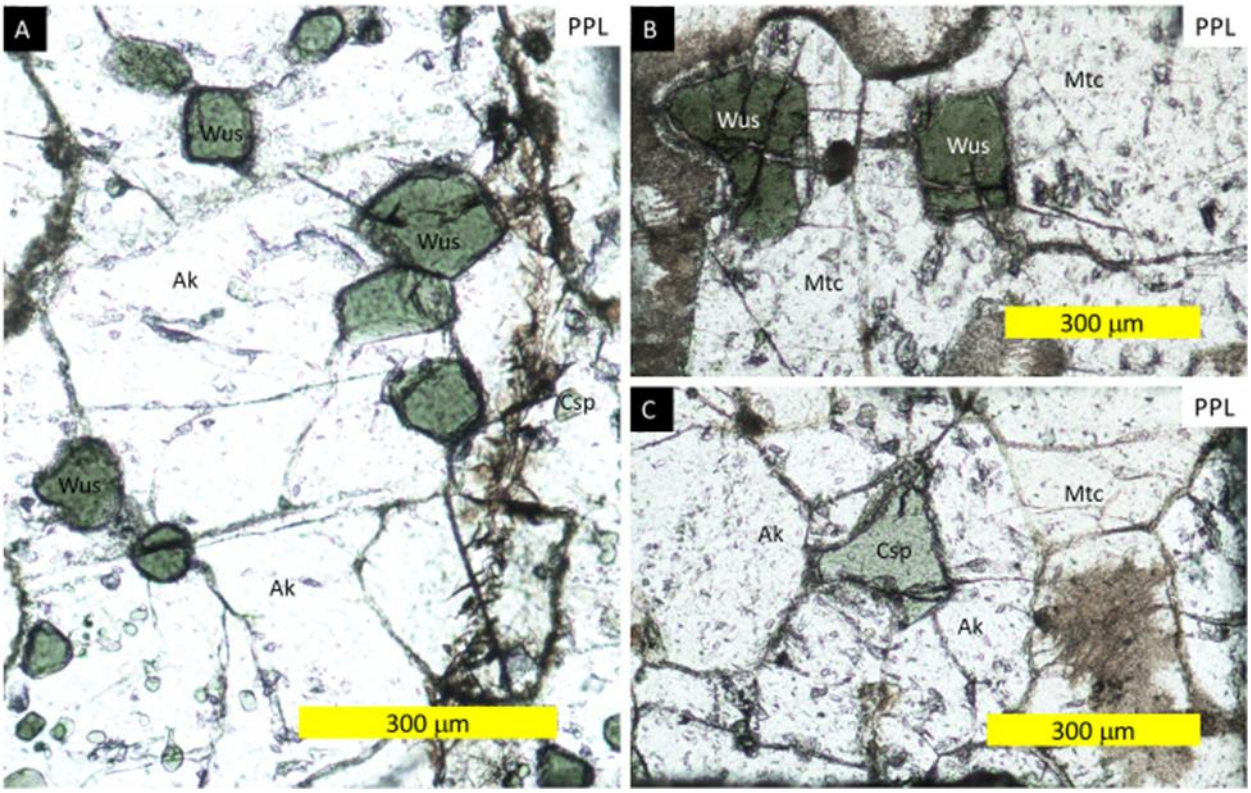

Figure 12: Micrographs of isolated grains of wüstite and chlorospinel for SEM from sample NF-02. Ak = Akermanite, Mtc = Monticellite, Wus = Wüstite, Csp = Chlorospinel

In the sample both wüstite and chlorospinel are present and have similar properties, both are isotropic and green in colour. Wüstite has a darker green colour, occasionally almost brown to opaque as seen in figure 12A, whereas the chlorospinel is slightly lighter in colour as seen in figure 12C. Both the wüstite and chlorospinel are less than 200µm is size and are included within the akermanite and monticellite. The wüstite in the sample seen in figure 12B is euhedral to subhedral and has a higher relief than the surrounding crystals, it makes up approximately 6% of the sample. The chlorospinel seen in figure 12C appears to less defined crystal shapes and lower relief than the wüstite, and only makes up 4% of the sample. It is likely that the chlorospinel formed after the wüstite and simultaneously with the melilite and monticellite allowing it to be included in the larger grains as well as filling space between them.

4.4 Sample NF-03

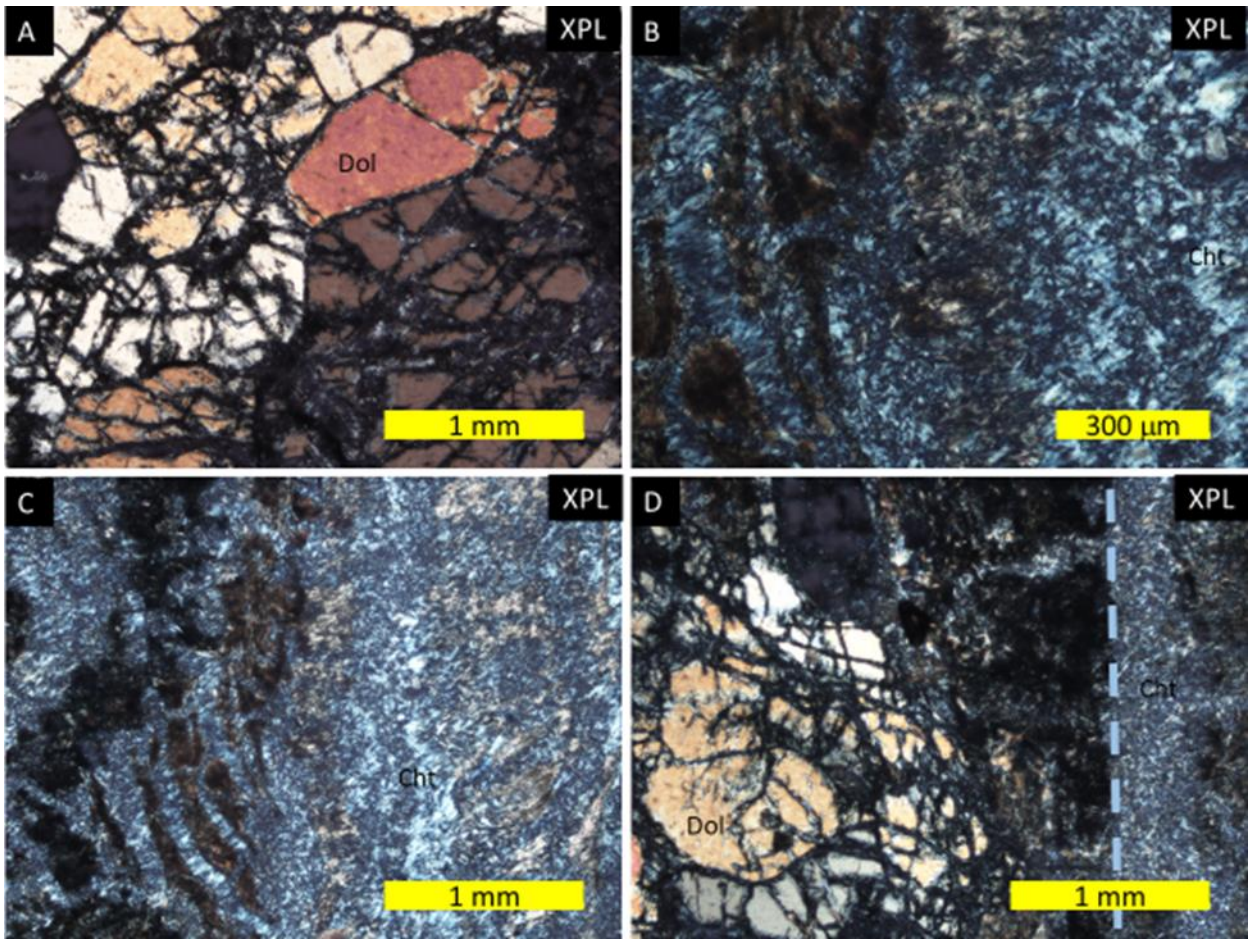

Figure 13: Micrographs of sample NF-03. Dol = Dolomite, Cht = Chert

Sample NF-03 is a metadolomite located within the calc-silicate package. Sample NF-03 has two textures: a highly fractured section with large grains, and a portion of very fine grain matrix. There is also a distinct boundary between the textures. Figure 13A shows the highly fractured, altered dolomite. The dolomite is present in large grains that have been sutured together in the dolomatising process, grains are larger than 1mm and 50% of the sample. In figures 13B,C there is a portion of the protodolomite that ~~bas~~has been broken up and is surrounded by the chert. The lineation present in the sample is marked by a distinct change in grain size as seen in Figure 13D. The other portion of the sample is made up of clay and altered chert clasts, the chert clasts are aphanitic and indistinguishable from each other.

4.5 Sample NF-04

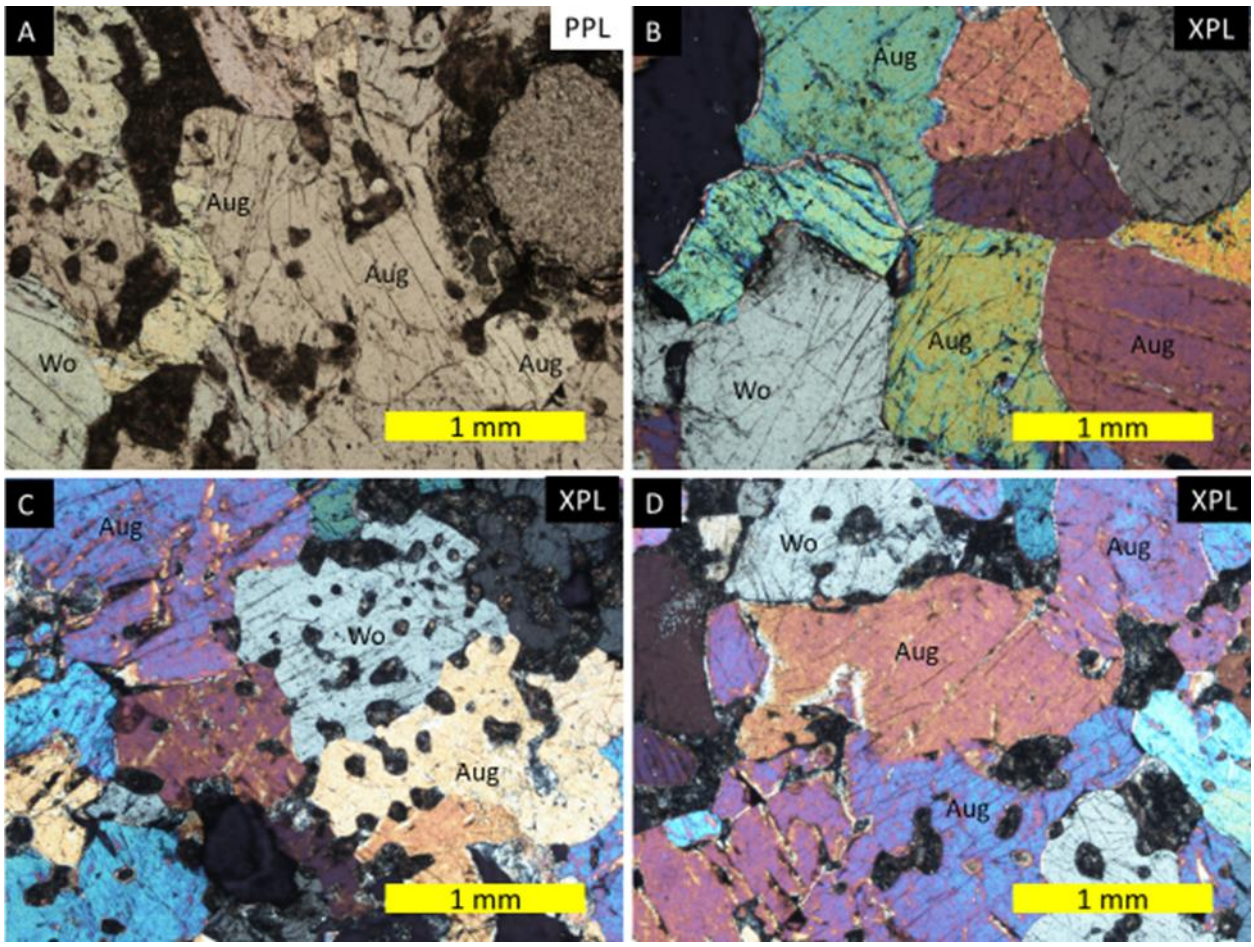

Figure 14: Micrographs of sample NF-04. Aug = Augite, Wo = Wollastonite

Sample NF-04 comes from the centre of the calc-silicate sheet, and is a metamorphosed pyroxenite[EB34] which most likely crystallised during metamorphism. In Figure 9, there is a dark layer in the centre of the package, and this is where the sample originated from. This sample contains large crystals, the majority of which are augite (70%) and wollastonite (25%) as seen in figures 14A,D. The crystals have similar relief but can be identified in the images based on birefringence, with wollastonite appearing as first-order greys and augite having second to third-order interference colours. The minerals in the sample are all large, most exceeding 1.5mm, subhedral to anhedral shape for the most part of the sample, figure 14B best displays the subhedral shape and figure 14D best displays the anhedral shape. In small sections as seen in Figure 14C, embayment of the minerals can be seen. [EB35]

4.6 Sample NF-05

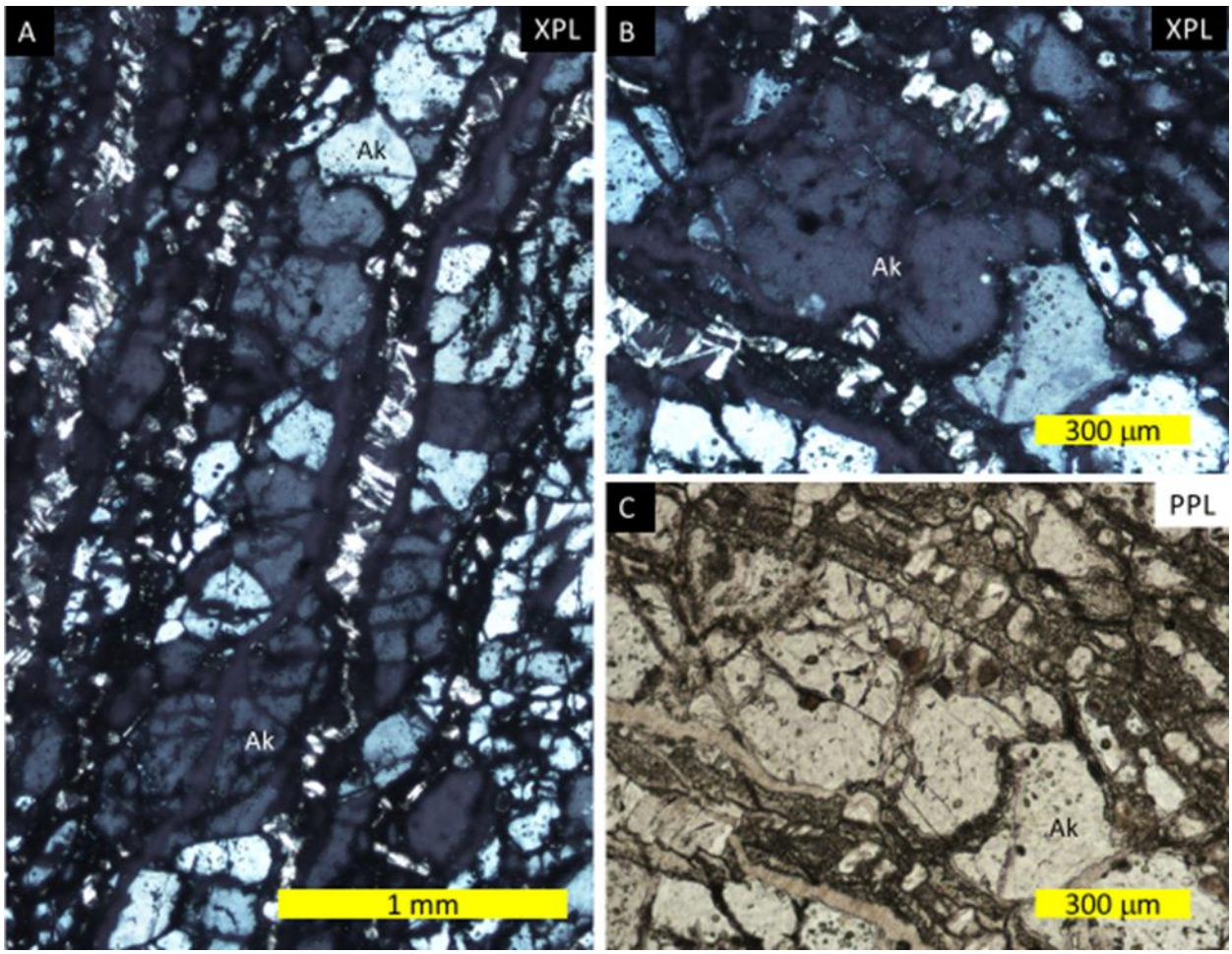

Figure 15: Micrographs of sample NF-05. Ak = Akermanite

This sample comes from the upper section of the sedimentary package, and is a metapelite. It consists predominantly of akermanite, approximately 85%, with minor interstitial minerals as seen in figures 15A. Figure 15B shows that the akermanite occurs as. medium to small grains between 1000µmm and 300µm [EB36]in size with a low first order birefringence colour. The grains are highly fractured and have a secondary mineral growth between the grains, the fractures can be seen more clearly in figure 15C. The sample shows foliation and the alignment of the akermanite this can be seen in a NNE-SSW orientation in figure 15A

4.7 Sample NF-06

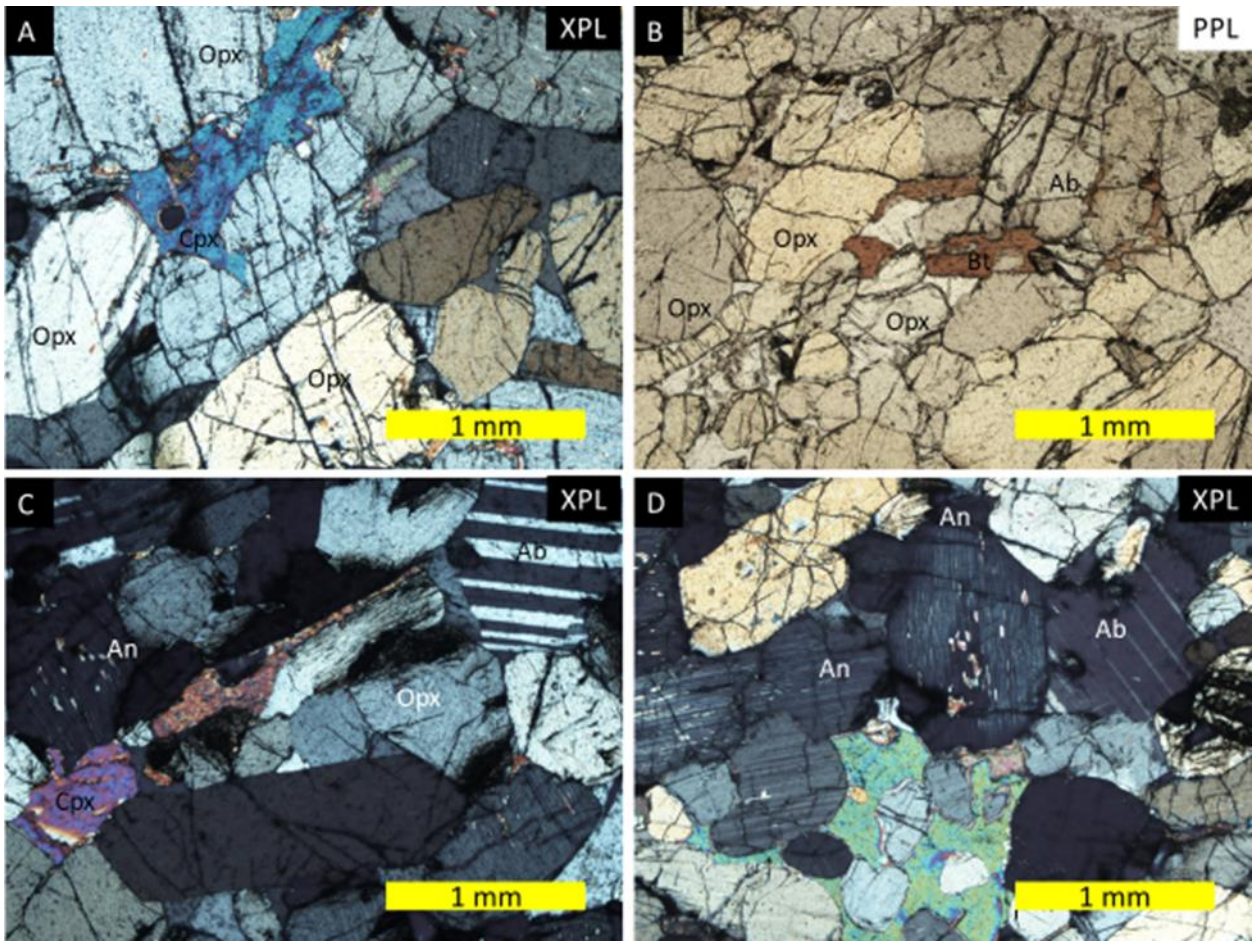

Figure 16: Micrographs of sample NF-06. An = Anorthite, Ab = Albite, Bt = Biotite, Cpx = Clinopyroxene, Opx = Orthopyroxene.

Sample NF-06 was taken from the host rock, and is a gabbronorite. The sample is made up mostly medium to large pyroxenes and feldspar crystals, with some minor micas present between crystals. The orthopyroxenes are subhedral and range in size from 0.5-2mm with an average around 1mm, and they make up 50% of the sample seen in figure 16A. The clinopyroxenes in the sample make up 10% and form in interstitial spaces seen in figure 16C. They are smaller than the orthopyroxenes and do not exceed 1mm. The plagioclase minerals are mostly euhedral to subhedral and are approximately 1mm in size on average seen in figure 16C,D. The feldspars make up the other large portion of the sample with 30%. The remainder of the sample consists of small interstitial minerals mostly micas like the biotite seen in Figure 16B. The sample shows distinct modal distribution with portions being predominantly populated by either pyroxene or feldspar.

5. Discussion

5.1 Mineralisation

The metamorphism of siliceous limestones and dolomite is more complex than most common metamorphic systems, in that it involves not only an H_2O fluid but instead an H_2O-CO_2 mix that evolves as the rock undergoes metamorphism (Spear, 1995). Considering the MgO present in the samples between 12 and 22 wt%, as seen in Table 1[EB37], the rock has undergone some degree of dolomitization before the metamorphism by the BIC occurred. The initial rock would have contained a portion of ferric dolomite resulting in a chemical system of CaO-SiO_2-MgO-FeO-CO_2-H_2O[EB38]. Spear (1995) lists the minerals commonly encountered with increasing degrees of metamorphism in such a system as talc followed by tremolite then diopside, forsterite and wollastonite then periclase, monticellite, akermanite with increasing temperature followed by tilleyite, spurrite, rankinite then merwinite and larnite. ~~Both~~ W[EB39]~~w~~üstite and chlorospinel are not common minerals in calc-silicate metamorphism, ~~; the presence of these minerals is due to another factor.~~ w~~W~~üstite is a FeO mineral; it is not common for Fe to be present in calc-silicates in such high quantities and is ~~subsequently~~ not largely considered when looking at calc-silicate metamorphism as it substitutes for Mg.~~,~~ [EB40]T~~therefore t~~he presence and abundance of Fe in the system may cause the formation of wüstite as well as the conditions that lead to the formation of chlorospinel.

According to Milodowski et al. (1989), the degassing of ferroan dolomite occurs above a temperature of 700ºC. Dolomite has two spikes in weight loss as the CO_2 is released whereas ferroan dolomite exhibits three steps of weight loss. The presence of iron in the system lowers the minimum temperature required the initiate degassing as well as making the weight loss more gradual than in pure dolomite. Warne et al. (1981) shows the first step of the degassing of dolomite peaks at 800ºC whereas with an increasing Fe % the temperature can be as low as 650ºC[EB41] at a pressure of 1 Kbar. ~~b~~[EB42]~~ecause~~ Because of the lower starting temperature of degassing in ferroan dolomites the process is more gradual with smaller spikes in CO_2 loss (Warne et al., 1981). [EB43][nf44]The three steps represent the following reactions;

Step 1: The decomposition of $MgCO_3$ and $FeCO_3$ to MgO, FeO and CO_2, followed by the oxidation of FeO forming Fe_2O_3

Reactions: $2Ca(Mg,Fe)(CO_3)_2 \rightarrow 2CaCO_3 + (Fe,Mg)O + 2CO_2$

$4FeO + O_2 \rightarrow 2Fe_2O_3$

$Fe_2O_3 + MgO \rightarrow MgFe_2O_4$

Step 2: The reaction between the Fe rich phase and the $CaCO_3$

Reactions: $CaCO_3 + Fe_2O_3 \rightarrow CaFe_2O_4 + CO_2$ or

$2CaCO_3 + Fe_2O_3 \rightarrow Ca_2Fe_2O_5 + 2CO_2$

Step 3: The remainder of the CaCO3 is broken down

Reaction: $CaCO_3 \rightarrow CaO + CO_2$

The decomposition reactions are complete by the time the samples reach 1000ºC, according to the testing done by Milodowski et al. in 1989. The tests done by Milodowski et al. (1989) where performed at ~~normal~~ atmospheric pressure~~s~~, it indicates that the temperature range for the metamorphism of the xenolith overlaps with the decomposition temperatures of between 700ºC and 1000ºC. The BIC is thought to have intruded at 1300ºC (Cawthorn and Walraven, 1998) with the surrounding contact areole being metamorphosed at pressures in excess of 5 kbar and temperatures up to 700ºC according to Waters and Lovegrove (2002). [EB45]The pressure the host rock was subjected to would most likely have been similar to the pressure that the slab was subjected to.

The presence of both wüstite and chlorospinel in sample NF-02 indicates unique conditions present ~~that occurred~~ [EB46]during the metamorphism of the rock. The wüstite in the samples indicates a lack of oxygen in the system; normally in this type of metamorphism the FeO is oxidised to Fe_2O_3 (Milodowski et al., 1989). There are two possibilities to explain the reduced nature of the Fe in the Dwarsrivier xenolith. First, it is possible that there was little to no free oxygen available in the system or being released during metamorphism. The other possibility is that the growth of other minerals enclosed the wüstite crystals and created a localised oxygen deficiency around the mineral grains. Nokleberg (1973) explains that at temperatures above 490ºC the reaction $3FeO + CO_2 = Fe_3O_4 + CO$ favours the production of CO, and that, due to the oxygen fugacity in a carbonate system, CO_2 does not readily break down to CO. Due to the fact that CO_2 does not break down, it does not release oxygen except for in the wüstite stability field, and this is the common reason for the lack of wüstite

preservation. Based on this information it is most likely that during the metamorphism of the calc-silicate rock that the release of oxygen occurs after the formation of wüstite. For the preservation of the wüstite, these crystals would need to be isolated from the available oxygen and there would need to be little movement of oxygen between solid phases. For this to happen the akermanite crystals would have to isolate the wüstite, which must have formed first, from the increased oxygen in the system. The isolation of the grains can be seen in figure 12 with wüstite grains being enclosed within other grains.~~.~~[EB47]

In contrast to wüstite that is preserved in the absence of O_2 the chlorospinel present in the sample is evidence of the oxidation of Fe^{+2} to Fe^{+3}, as chlorospinel requires Fe^{+3} to form (Bothwell and Hey, 1958). According to Sabine et al. (1968), Fe[EB48]$^{+3}$ more commonly substitutes into the Al^{+3} site in the lattice rather than the Mg^{+2} which results in ferroan chlorospinel, Mg(Al, Fe[EB49]$^{+3}$)$_2O_4$. The spot analysis in table 3 display FeO values in excess of 6 wt%, and the Fe has most likely, therefore, been oxidised in the system; this must have occurred after the formation or isolation of the wüstite. The chlorospinel shows that there was free oxygen in the system, but as it is rare in the sample, it also indicates that there was not an abundance of oxygen and the oxidation of the Fe was relatively small and localised. If the wüstite found in the sample is solely due to the isolation of the grains from the oxygen available in the system, then the ferroan dolomite would have devolatilised as proposed by Milodowski et al. (1989). For this to have occurred the temperatures that the rock would have experienced would have been in excess of 700ºC allowing for the degassing, and formation of the wüstite and the oxidisation of the Fe in the rock.

Chlorospinel is a mineral that forms predominantly in skarn like deposits where carbonates, enriched in aluminium and magnesium, are subjected to contact metamorphism. An example of this is in Predazzo-Monzoni, Italy where Princivalle et al. (1999) describe a dolomitic area that was subjected to mafic magmatism with low pressures, less than 1 kbar, and temperatures from 400ºC to 700ºC which resulted in a mineral assemblage containing chlorospinel. In Iraq samples containing chlorospinel have also been found and described by Al-Hermezi et al. (1986), in a similar environment that is adjacent to diorite intrusions and has undergone high degrees of thermal metamorphism [EB50]as well as hydrothermal alteration with temperatures of approximately 770°C and pressures up to 1 kbar.

Wüstite occurs very rarely in nature as the high temperatures and low oxygen fugacity required for stable formation are not common in crustal settings. Most common examples of wüstite occur in labs or the production of iron. O~~There is o~~ne example of natural wüstite is in

Idaho, USA, described by Nadoll and Mauk (2011) present in hydrothermal veins. It is described as non-stoichiometric wüstite as it is not pure Fe^{2+} containing some Fe^{3+} and is presumed to have formed at lower than optimal temperatures, below 570ºC, as above these temperatures wüstite forms as pure Fe^{2+}. In the example found by Nadoll and Mauk (2011) the wüstite is in a gauge of siderite with calcite present indicating a carbonate source. The source is thus similar to that found in the Dwarsrivier Pass, a metamorphically altered carbonate rock resulting in a reducing environment. In the Czech Republic, wüstite was found in an S-type granite which is the first recorded finding of wüstite in a granite (Seifert et al., 2010). In this example, the formation was facilitated by graphite which lowered the overall oxygen fugacity within the magma.

A pseudosection for sample NF-02 was constructed with PERPLE_X [EB51]using the computational model from Connolly and Petrini (2002) and the data file hp62ver.dat [EB52]from Holland and Powell (2011)~~data file~~. Multiple variations were created with different variables~~iations~~[EB53]~~,~~ and the most appropriate pseudosection was selected (figure 17) the log for the generation of the pseudosection can be found in the appendix[EB54]. The selected pseudosection showed the most similarity to the sample assemblage while remaining in the plausible region for the P-T conditions. Due to the unconventional if not unique assemblage in the sample, the pseudosection is not considered accurate, but does indicate the general range of temperatures that likely affected the sample. The pseudosection lacks both the presence of wüstite and chlorospinel, arguably the key minerals in the sample, but it was possible to model the presence of a spinel phase as well as Fe-periclase. Periclase and [EB55]wüstite are part of a solid solution series, so Fe-periclase is taken as a proxy for wüstite.

Fe-periclase and monticellite form at relatively low temperatures in the pseudosection, but akermanite only forms at temperatures above 1013ºC. The Fe-periclase/ wüstite -growth does not match the initial temperature predictions (500ºC), as it is shown to form before the degassing temperature of dolomite,700ºC, which may be the reason the iron remains in a 2+ state. The spinel only forms at low temperatures and could only have formed after the oxidation of the Fe^{+2} to Fe^{+3}, so, this must have occurred ~~regressively~~ a[EB56]s the rock cooled after the heating. The pseudosection calculates mineral phases that are not present in the sample, such as vesuvianite ($Ca_{19}Mg_2Al_{11}Si_{18}O_{69}(OH)_9$), gehlenite ($Ca_2Al_2SiO_7$), brucite ($Mg(OH)_2$) and hercynite ($FeAl_2O_4$). While the mineral assemblage of the sample is not exactly the same as that of the pseudosection, the section does shed light on the formation of akermanite.

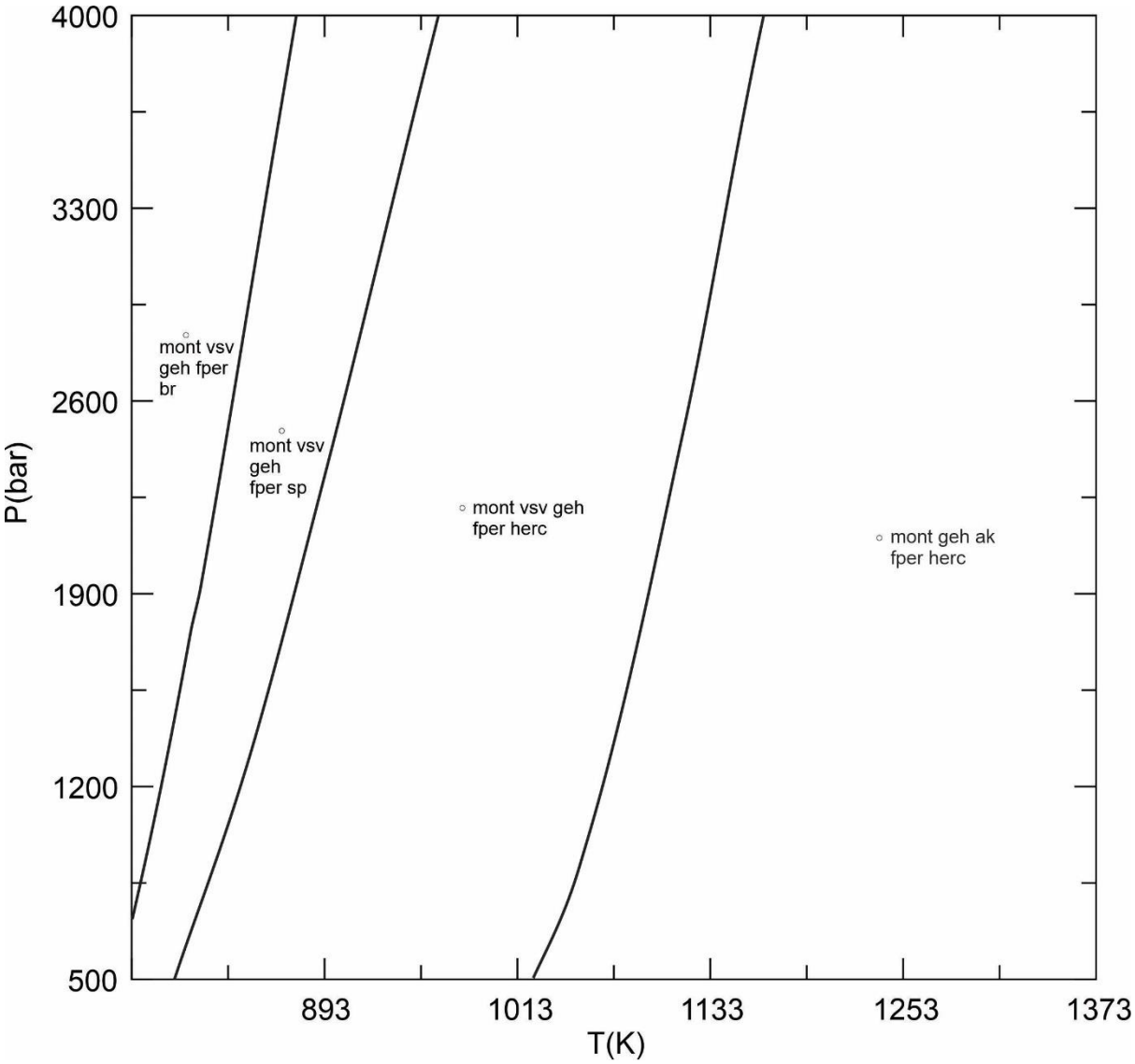

Figure 17: Pseudosection for sample NF-02. Mont = Monticellite, Vsv = Vesuvianite, Geh = Gehlenite, Fper = Fe-periclase, Br = Brucite, Sp = Spinel, Herc = Hercynite.

5.2 Formation

The only current formational model for the Dwarsrivier Pass outcrop is suggested by Clarke et al. (2005). After studying the modal layering as well as the orientational offset between this section of the Critical Zone and the Main Zone within the RLS, Clarke et al. (2005) concluded that the area is host to a sheath fold capped by the layer of competent calc-silicate rock. The deformation in the area is attributed to post intrusion diapirism, a model in which the origin and state of the calc-silicate is a result of the diapiric rise of magma bringing the xenolith up from the underlying Pretoria Group.

The issues with this theory is the competency of the calc-silicate, the need to withstand the temperature of the rising magma as well at the large distance required for the xenolith to have travelled. The temperature is not considered a problem due to a process called “cold-diapirism” reported by Gerya et al. (2003) in which density drives the diapirism opposed to heat; this would account partially for the preservation of the calc-silicate (Clarke et al., 2005). As for the distance travelled by the xenolith, towards the outskirts of the BIC, the RLS it~~[EB57]~~ is thinner in cross-section, this could mean that the xenolith did not travel through the entirety of the RLS and then the folding action uplifted the xenolith (Clarke et al., 2005).

An alternative formational model proposed in this project is delamination of the roof in the magma chamber of the Critical Zone. If the calc-silicate package is indeed a delaminated piece of roof, it would account for the competence of the slab as it would not have travelled very far or have been subjected to turbulent upliftment through the RLS. The model for formation can be seen in figure 18. The delamination would have occurred after the Critical Zone had begun to cool indicated by the lower portion of the slab where wüstite is present, having been subjected to higher temperatures than the upper portion.

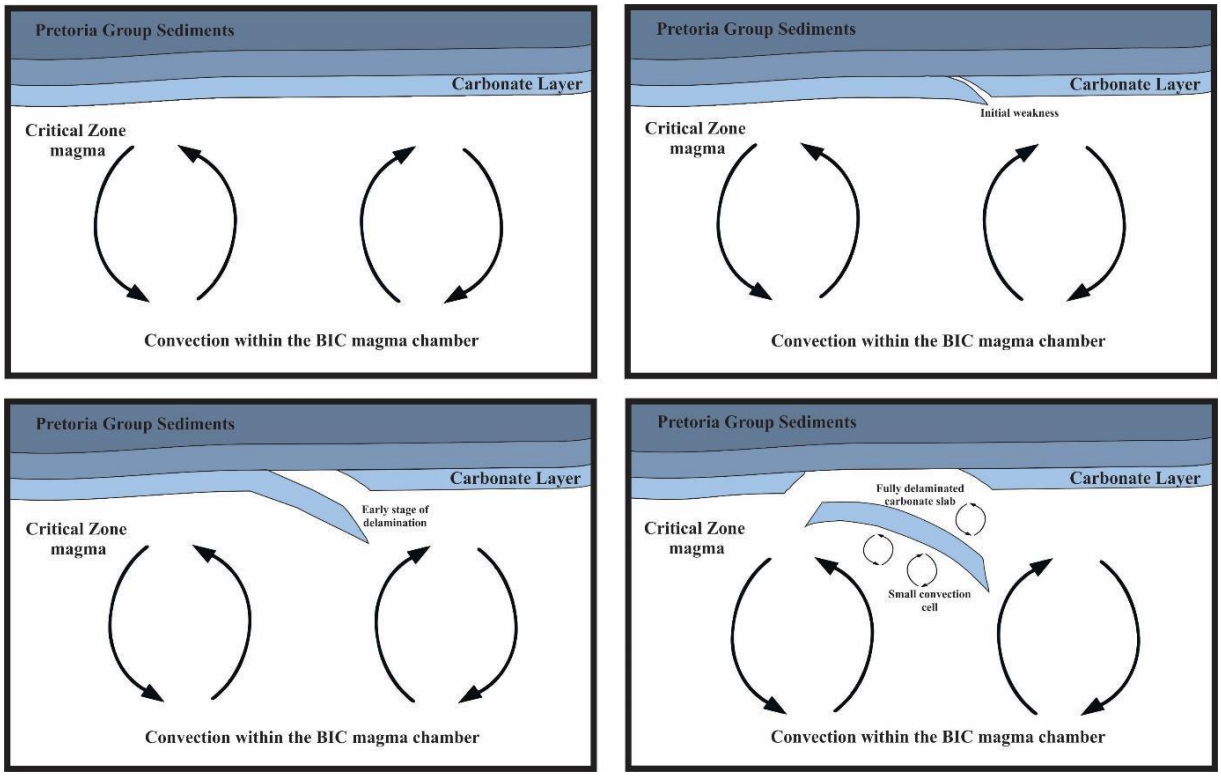

Figure 18: Model displaying the delamination of the roof slab.

The weakness in the roof which led to the delamination may have been a result of the loss of upward hydraulic pressure caused by a hiatus or the termination of new magma rising up (Aragon et al., 2019). It is possible that magma was no longer pushing up but instead extending laterally also resulting in a loss of upward hydraulic pressure (Aragon et al., 2019). This loss of pressure is the same effect that leads to the formation of laccoliths and calderas according to Aragon et al. (2019); in the case of the delaminated roof slab in question the convection within the Critical Zone would have aided to the delamination and subduction of the slab similar to a subducting tectonic plate. Helz (2009) describes convection cells in mafic magma chambers similar to diapiric rise, and it is also recorded that the presence of dissolved volatiles such as H_2O or in the case of the calc-silicate slab CO_2 + H_2O liquid phase and the temperature range extends before the plagioclase phase begins to crystallise. This may be what caused the slab to subducted into a slightly cooler but still ductile and partially liquid magma chamber.

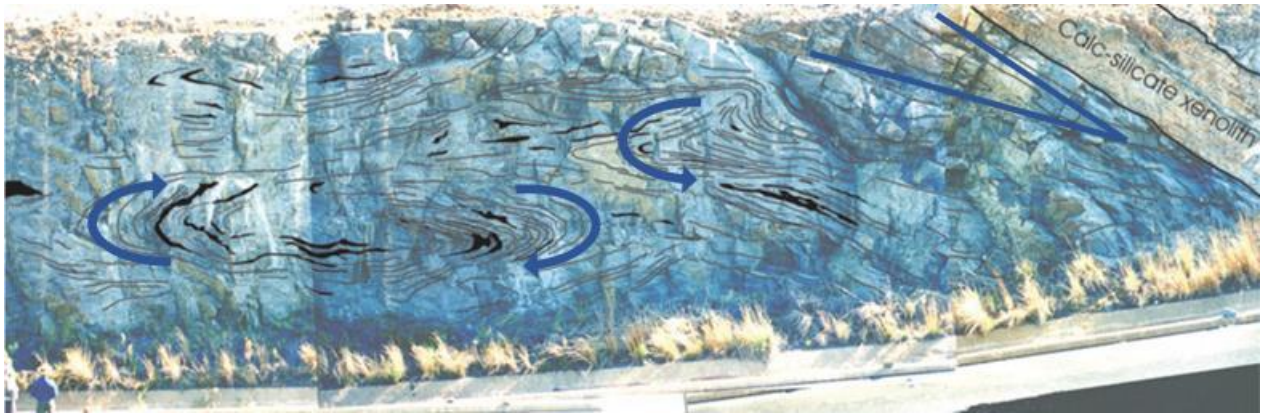

Figure 19: Composite image of the folds and calc-silicate slab modified from an image published by Clarke et al. (2005).

There are structures in the surrounding host rock described by Clarke et al., (2005) as folds; these suggested folds may have another origin. These folds can be seen in figure 19; the folds have multiple orientations as seen in this image which is mirrored in the stereographic data posed by Clarke et al. (2005). Clarke et al. (2005) identified three unique fold axes for the small-scale folds on the outcrop with one of these axes correlating to the large-scale fold proposed for the area. It is possible that the “swirl structures” are preserved

convection cells; the nature of the convection cells can be seen indicated in figure 19 with blue arrows towards the left-hand side of the image. Towards the right side of the image where the slab can be seen there is a differently orientated fold this is likely due to the cold slab terminating the convection cells and moving the crystal mush with it as it subducted.

The swirl structures and the modal distribution of pyroxenes are a result of the subducting roof slab. The semi-crystalline mush created by the devolatisation of the calcium carbonates would have allowed the early forming pyroxenes to accumulate in layers within the mush. The pyroxene layers could then have been disturbed by the slab creating smaller turbulent convection cells as it sank; these cells may be partially preserved in the outcrop. The convection may be the reason Clarke et al. (2005) identified three main fold orientations within the rock in the Dwarsrivier Pass portion of the Critical Zone.

5.3 Protolith

The sheet itself extends laterally in a NE-SW direction visible in a quarry adjacent to the road cutting indicating that it is of a relatively large scale and laterally continuous. The section of rock is approximately 2m thick with varying degrees of weathering. Due to the samples being of a calc-silicate nature, ~~considering~~ the majority of the samples contain in excesses of 30 wt% SiO_2 and 20 wt% CaO (Table 1), there are a few possible protoliths for the metamorphism. The protolith was most likely made up of multiple thin layers of carbonate which may have varied in composition.

The main sedimentary packages to consider within the Pretoria Group are those that contain limestone, marble or dolomite due to the abundance of Ca present; there are only two formations in the Pretoria Group that contain layers of carbonate rock that could be the protolith for the rock in question. The first formation is the Vermont Formation, and the second is the Nederhorst Formation. The only other source of carbonate rock large enough is in the Chuinespoort Group below the Pretoria Group (Schrieber and Eriksson, 1992). The Chuniespoort Group is too low in the stratigraphy to be a source for the rock and is not in contact with the RLS. The Chuinespoort Group also contains thick layers of dolomite interlayered with chert which do not match the thinner layers observed in the sedimentary slab.

The Vermont Formation is the tenth formation in the Pretoria Group and has three portions that contain carbonate rocks described as localised occurrences by Button (1976). The carbonate rocks of the Vermont Group have commonly undergone metamorphism with the recorded rocks being marble, serpentinized dolomite and calc-silicate rocks (Schrieber and Eriksson, 1992). [EB58]The Nederhorst Formation is the twelfth formation in the Pretoria Group, making it higher in the sequence that the Vermont and subsequently closer to where the BIC intruded (Eriksson et al., 1993). The Nederhorst Formation contains layers of calc-silicate rock that can be up to 5m thick. In most cases the carbonate rocks of the Nederhorst host dykes and display varying degrees of metamorphism (Button, 1976).

Based on the proposed formational modal in this thesis of the two probable sources within the Pretoria Group the Vermont Formation looks promising but lacks the sheer volume of material required for the slab. The Nederhorst Formation has thicker beds of calcium carbonate-rich rock as well as being stratigraphically closer to the top of the intrusion. The Nederhorst Formation is the most plausible source for the metamorphosed slab, and it is also more in line with the slab delaminating and subducting opposed to being brought up from below, through the intrusion.

6. Conclusion

Based on the evidence provided, it is likely that the magma chamber was in a liquid or partially liquid phase and subsequently over 850ºC. The chamber would most likely be under pressures around 5 kbar based on previous studies and the partial pressure of the released CO_2. The calc-silicate was subjected to temperatures in excess of 700ºC for the degassing of the volatiles to occur, the degassing is evident in the formation and preservation of ferrous chlorospinel which requires the presence of the released O_2 to form. The preservation of wüstite in sample NF-02 is a result of an initial phase of metamorphism in which oxygen was not as readily available to oxidise the iron, and these crystals were then preserved in akermanite crystals which enclosed them. It can be noted that the lower portion of the calc-silicate slab was subjected to higher temperatures before the slab was subducted, as indicated by the presence of olivine and clinopyroxene crystals which only occur in the bottom portion of the rock. The difference in metamorphism indicates that the BIC was initially at a temperature greater than that which metamorphosed the remainder of the rock.

For the origin of the calc-silicate rock there are two probable sources within the Pretoria Group, the Vermont Formation looks promising but lacks the sheer volume of material required for the slab. The Nederhorst Formation has thicker beds of calcium carbonate-rich rock as well as being closer lithological to the top of the intrusion. The Nederhorst Formation is the plausible source for the metamorphosed slab, and it is also more in line with the slab subducting opposed to being brought up from below, through the intrusion.

The source of the rock, as well as the varying degrees of metamorphism, are the dominant reasoning behind the proposed formational model. If the rock were transported through the BIC, it would have higher degrees of metamorphism throughout. Instead, the areas of high metamorphism are localised in the lower portion. It, therefore, resulted in the theory of the calc-silicate package being situated in the roof rock and delaminating from this position. The delamination resulted in a slab which was then subducted into the magma chamber which was in a ductile state, evident by the swirled nature of the modal distribution of pyroxene crystals in this portion of the BIC.

Bibliography

Al-Hermezi, H. M., McKie, D. & Hall, A. J., 1986. Baghdadite, a New Calcium Zirconium Silicate Mineral From Iraq. *Mineralogical Magazine,* Volume 50, pp. 119-123.

Aragon, E. et al., 2019. Magma Chamber Growth Models in the Upper Crust: A Review of the Hydrolic and Inertial Constraints. *Geoscience Frontiers* , Volume 10, pp. 1211-1218.

Barnes, S.-J. & Maier, W. D., 2002. Platinum-Group Element Distributions in the Rustenburg Layered Suite of the Bushveld Complex, South Africa. *The Geology, Geochemisty, Mineralogy and Mineral Benefication of Platinum-Group Elements* , Volume 54, pp. 431-458.

Bothwell, D. & Hey, M., 1958. The Nature of Chlorospinel. *Mineralogical Magazine and Journal of the Mineralogical Society,* Issue 31(241), pp. 885-887.

Button, A., 1976. Stratigraphy and Relations of the Bushveld Floor in the Eastern Transvaal. *Trans. Geol. Soc. S. Afr,* 1(79), pp. 3-12.

Catuneanu, O. & Eriksson, P. G., 2002. Sequence Stratigraphy of the Precambrian Rooihoogte- Timeball Hill Rift Succession, Transvaal Basin, South Africa. *Sedimantary Geology* , Volume 147, pp. 71-88.

Cawthorn, R. G. & Walraven, F., 1998. Emplacement and Crystallization Time for the Bushveld Complex. *Journal of Petrology,* 39(9), pp. 1669-1687.

Cawthorn, R. G. & Webb, S., 2013. Cooling of the Bushveld Complex, South Africa: Implications for Palemagnetic Reversals. *Geology published online* .

Cheney, E. S. & Twist, D., 1991. The Conformable Emplacement of the Bushveld Mafic Rocks Along a Regional Unconformity in the Transvaal Succession of South Africa. *Precambrian Research,* Volume 52, pp. 115-132.

Clarke, B. M., Uken, R., Watkeys, M. K. & Reinhardt, J., 2005. Folding of the Rustenburg Layered Suite Adjacent to the Steelpoort Pericline: Implications for Syn-Bushveld Tectonism in the Eastern Bushveld Complex. *South African Journal of Geology,* Volume 108, pp. 397-412.

Connolly, J. & Petrini, K., 2002. An Autimated Stratergy for Calculation of Phase Diagram Sections and Retrieval of Rock Properties as a Function of Physical Conditions. *Journal oF Metamorphic Petrology,* Volume 20, pp. 697-708.

Draken, L. S. & Gurry, R. W., 1945. The System Iron-Oxygen I. The Wustite Field and Related Equilibria. *Journal of American Chemical Society*, 67(8), pp. 1398-1412.

Eales , H. V. et al., 1993. The Mafic Rocks of the Bushveld Complex: a Review of Emplacement and Crystallization History, and Mineralization, in the Lite of Recent Data. *Journal of African Earth Science* , 16(1/2), pp. 121-142.

Eales, H. V. & Cawthorn, R. G., 1996. The Bushveld Complex. In: R. G. Cawthorn, ed. *Layered Intrusions.* Amsterdam: Elsevier, pp. 181-225.

Eriksson, P. G. et al., 2001. Major Influences on the Evolution of the 2.67- 2.1 Ga Transvaal Basin, Kaapvaal Craton. *Sedimentary Geology* , Volume 141-142, pp. 205-231.

Eriksson, P. G., Hattingh, P. J. & Altermann, W., 1995. An Overview of the Geology of the Transvaal Sequence and Bushveld Complex, South Africa. *Mineralium Deposita,* Volume 30, pp. 98-111.

Eriksson, P. G., Meyer, R. & Botha, W. J., 1988. A Hypothesis on the Nature of the Pretoria Group Basin. *S. Afr. Tydskr. Geol.,* 91(4), pp. 490-497.

Eriksson, P. G., Nixon, N. & Snyman, C. P., 1987. A Study of Upper Pretoria Group Sedimentary Rocks in Contact with the Rustenburg Suite in the Buffelspoort Dam Area, Near Rustenburg. *S. Afr. Tydskr. Geol.,* 90(2), pp. 124-136.

Eriksson, P. G. et al., 1995. Architectural Element from Lower Proterozoic Braid-delta and High-energy Tidal Flat Deposits in the Magaliesberg Formation, Transvaal Supergroup, South Africa. *Sedimentary Geology* , Volume 97, pp. 99-117.

Eriksson, P. G. et al., 1993. The Transvaal Sequence: an Overview. *Journal of African Earth Science* , 16(1/2), pp. 25-51.

Eriksson, P. G., Twist, D., Snyman, C. P. & Burger, L., 1990. The geochemistry of the Silverton Shale Formation, Transvaal Sequence. *South African Journal of Geology* , 93(3), pp. 454-462.

Hofmann, A., 2014. Transvaal Supergroup, South Africa. *Encyclopedia of Astrobiology* .

Holland, T. & Powell, R., 2011. An Improved and Extended Internally Consistent Thermodynamic Dataset for Phase of Petrographical Intrest, Involving a New Equation of State for Solid. *Journal for Metamorphic Geology*, Volume 29, pp. 333-383.

Kaneko, Y., Tsunogea, T. & Miyano, T., 2005. Crystal-size Distribution of Garnets in Metapelites from the Northeastern Bushveld Contact aureole, South Africa. *American Mineralogist,* Volume 90, pp. 1422-1433.

Kinnaird, J. A., 2005. The Bushveld Large Igneous Province. *School of Geoscience, University of Witwatersrand.*

Kleemann, G. J. & Twist, D., 1989. The Compositionally-zoned Sheet-like Granite Pluton of the Bushveld Complex: Evidence Bearing on the Nature of A-type Magmatism. *Journal of Pertology* , Volume 30, pp. 1383-1414.

Latypov, R., Chistyakova, S., Page, A. & Hornsey, R., 2016. Field Evidence for the In Situ Crystallization of the Merensky Reef. *Journal of Petrology*, Volume 56, pp. 2341-2372.

Lenhardt, N., Eriksson, P. G., Catuneanu, O. & Bumby, A. J., 2012. Nature of and Controls on Volcanism in the ca. 2.32-2.06 Ga Pretoria Group, Transvaal Supergroup, Kaapvaal Craton, South Africa. *Precambrian Research,* Volume 214-215, pp. 106-123.

Milodowski, A. E., Morgan , D. J. & Warne, S. S. J., 1989. Thermal Analysis Studies of the Dolomite-Ferroan Dolomite-Ankerite Series. II. Decomposition Mechanism in Flowing CO, Atmosphere. *Thermochimica Acta,* Issue 142, pp. 279-297.

Molyneux, T. G., 1974. A Geological Investigation of the Bushveld Complex in Sekhukhuneland and Part of the Steelpoort Valley. *Trans. Geol. Soc. S. Afr.*, Issue 77, pp. 329-338.

Moore, J. M., Tsikos, H. & Polteau, S., 2001. Deconstructing the Transvaal Supergroup, South Africa: Implications for Palaeoproterozoic Palaeoclimate Models. *Journal of African Earth Science* , Volume 33, pp. 437-444.

Nadoll, P. & Mauk, J. L., 2011. Wustite in a Hydrothermal Silver-Lead-Zinc Vein, Lucky Friday Mine, Coeur d'Alene Mining District, U.S.A.. *American Mineralogist,* Volume 96, pp. 261-267.

Nell, J., 1985. The Bushveld Metamorphic Aureole in the Potgietersrus Area: Evidence for a Two-Stage Metamorphic Event. *Economic Geology* , Volume 50, pp. 1129-1152.

Nokelberg, W. J., 1973. CO2 as a Source of Oxygen in the Metasomatism of Carbonates. *American Journal of Science* , Volume 273, pp. 498-514.

Parizot, M. et al., 2006. Suspected Microbial Mat-Related Crack-Like Sedimentary Structures in the Palaeproterozoic Magaliesberg Formation Sandstone, South Africa. *openUP*.

Princivalle, F., Della Giusta, A., De Min, A. & Piccirillo, E. M., 1999. Crystal Chemistry and Significance of Cation Ordering in Mg-Al Rich Spinels From High-Grade Hornfels (Predazzo-Monzoni, NE Italy). *Mineralogical Magazine* , 62(2), pp. 257-262.

Raubenheihmer, D., 2012. *P-T Estimates of Peak Bushveld Metamorphism in the Eastern Bushveld Complex, Limpopo Province, South Africa: Constraints from P-T Pseudosections.* Pretoria : University of Pretoria .

Reczko, B. F. F., Eriksson, P. G. & Snyman, C. P., 1995. Some Evidence for the Base-metal Potential of the Pretoria Group: Stratigraphic Targets, Tectonic Setting and REE Patterns. *Mineralium Deposita*, Volume 30, pp. 162-167.

Sabine, P. A., Sergeant, G. A. & Young, B. R., 1968. *Ferrian Chlorospinel from Carneal, Co. Antrim.* London: Institute of Geological Science, London.

SACS, 1980. Part 1: Lithostratigraphy of the Republic of South Africa. In: L. E. Kent, ed. *Geological Survey Stratigraphy of South Africa, Handbook 8.* s.l.:Government Printer, p. 690.

Scheiber, U. M. & Eriksson, P. G., 1992. The sedimentology of the Post-Magaliesberg Formation of the Pretoria Group, Transvaal Sequence, in the Eastern Transvaal. *South African Journal of Geology* , 95(1/2), pp. 1-16.

Schreiber, U. M., Eriksson, P. G. & Snyman, C. P., 1992. Mudrock Geochemistry of the Proterozoic Pretoria Group, Transvaal Sequence (South Africa): Geological Implications. *Journal of African Earth Science* , 14(3), pp. 393-409.

Schweitzer, J. K., Hatton, C. J. & de Waal, S. A., 1995. Regional Lithochemical Stratigraphy of the Rooiberg Group, Upper Transvaal Supergroup: A Proposed New Subdivision. *South African Journal of Geology*, 98(3), pp. 245-255.

Seifert, W., Thomas, R., Rhede, D. & Forster, H., 2010. Origin of Coexisting wustite, Mg-Fe and REE Phosphate Minerals in Graphite-Bearing Fluorapatite From the Rumburk Granite. *European Journal or Mineralogy,* Volume 22, pp. 495-507.

Spear, F. S., 1995. *Metamorphic Phase Equilibria and Pressure-Temperature-Time Paths.* 1st ed. Washington D.C.: Mineralogical Society of America.

Twist, D. & French, B. M., 1983. Voluminous Acid Volcanism in the Bushveld Complex: a Review of the Rooiberg Felsite. *Bulletin of Volcanology*, 46(3), pp. 225-242.

Wallmach, T., Hatton, J., De Waal, S. A. & Gibson, R. L., 1995. Retrogressive Hydration of Calc-silicate Xenoliths in the Eastern Bushveld Complex: Evidence for Late Magmatic Fluid Movement. *Journal of African Earth Science* , 21(4), pp. 633-646.

Walraven, F., 1985. Genetic Aspects of the Granophyric Rocks of the Bushveld Complex. *Economic Geology*, Volume 50, pp. 1166-1180.

Walraven, F., Armstron, R. A. & Kruger, F. J., 1990. A Chronostratigraphic Framework for the North-Central Kaapvaal Craton, the Bushveld Complex and the Vredefort Structure. *Tectonophysics*, Volume 171, pp. 23-48.

Warne, S. S. J., Morgan, D. J. & Milodowski, A. E., 1981. Thermal Analysis Studies of the Dolomite, Ferroan Dolomite, Ankerite Series. Part 1. Iron Content Reacognition and Determination by Variable Atmosphere DTA. *Thermochemica Acta*, pp. 105-111.

Waters, D. J. & Lovegrove, D. P., 2002. Assessing the Extent of Disequilibrium and Overstepping of Prograde Metamorphic Reactions in Metapelites from the Bushveld Complex Aureole, South Africa. *Journal of Metamorphic Geology*, Volume 20, pp. 135-149.

Willemse, J., 1969. The Geology of the Bushveld Igneous Complex, the Largest Repository of Magmatic Ore Deposits in the World. *Economic Geology Monograph*, Volume 4, pp. 1-22.

Wilson, J., Ferre, E. C. & Lespinasse, P., 2000. Repeated Tabular Injection of High-Level Alkaline Granites in the Eastern Bushveld, South Africa. *Journal of the Geological Society, London*, Volume 157, pp. 1077-1088.

Zeh, A., Ovtcharova, M., Wilson, A. H. & Schaltegger, U., 2015. The Bushveld Complex was Emplaced and Cooled in less than One Million Years - Results of Zirconology, and Geotectonic Implications. *Earth and Planetary Science Letters*, Volume 418, pp. 103-114.

Appendix

Perple_X Log

Run Build

Output file name: Pseudosection 8

Thermodynamic data file: hp62ver.dat

Computational option file: default = perplex_option.dat

Database components: unaltered

Saturated fluid: H2O, CO2

Saturated components: None

Chemical potentials, activities or fugacities as independent variables: None

Thermodynamic components in set: SiO2, FeO, MgO, CaO, MnO, Al2O3

Fluid equation state: X(CO2) H2O-CO2 CORK Holland & Powell 91, 98

Computational mode: Constrained minimization on a 2d grid

Pressure and Temperature relationship: independent variables

Set x-axis: T

Set minimum temperature (K): 773

Set Maximum temperature (K): 1373

Set y-axis: P

Set minimum pressure (bar): 500

Set maximum pressure (bar): 5000

Specific sectioning value for Y(CO2): 0

Specific component by weight: yes

Weight imputed as per table 1, sample NF-02

Output print file: yes

Exclude pure endmember phases: yes

Prompted for phases: no

Excluded phases: rnk, lrn, wo, merw, chum, cumm, cpv

Solution models included: none

Calculation title: pseudosection8

Run Vertex

Input: pseudosection8

Run Pssect

Input: psuedosection8

Modifications: none